8 Magnetism

8.1 Introduction

The topic of this part of the lecture deals are the magnetic properties of materials. Most materials are generally considered to be "non-magnetic", which is a loose way of saying that they become magnetized only in the presence of an applied magnetic field (dia- and paramagnetism). We will see that in most cases these effects are very weak, and the magnetization is lost, as soon as the external field is removed. Much more interesting (also from a technological point of view) are those materials, which not only have a large magnetization, but also retain it even after the removal of the external field. Such materials are called *permanent magnets* (ferromagnetism). The property that like (unlike) poles of permanent magnets repel (attract) each other was already known to the Ancient Greeks and Chinese over 2000 years ago. They used this knowledge for instance in compasses. Since then, the importance of magnets has risen steadily. Now they play an important role in many modern technologies:

- *recording media (e.g. hard disks)*: data is recorded on a thin magnetic coating. The revolution in information technology owes as much to magnetic storage as to information processing with computer chips (i.e. the ubiquitous silicon chip).

- *credit, debit, and ATM cards*: all of these cards have a magnetic strip on one side.

- *TVs and computer monitors*: contain a cathode ray tube that employs an electromagnet to guide electrons to the screen. Plasma screens and LCDs use different technologies.

- *speakers and microphones*: most speakers employ a permanent magnet and a current-carrying coil to convert electric energy (the signal) into mechanical energy (movement that creates the sound).

- *Electric motors and generators*: some electric motors rely upon a combination of an electromagnet and a permanent magnet, and, much like loudspeakers, they convert electric energy into mechanical energy. A generator is the reverse: it converts mechanical energy into electric energy by moving a conductor through a magnetic field.

- *Medicine*: Hospitals use magnetic resonance imaging to spot problems in a patient's organs without invasive surgery.

- *fridge magnets*

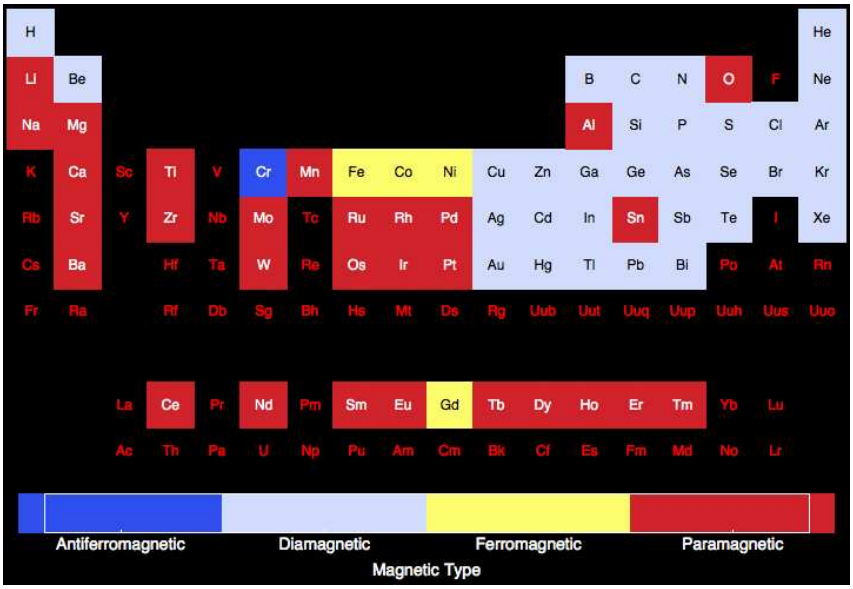

Figure 8.1: Magnetic type of the elements in the periodic table. For elements without a color designation magnetism is even smaller or not explored.

Figure 8.1 illustrates the type of magnetism in the elementary materials of the periodic table. Only Fe, Ni, Co and Gd exhibit ferromagnetism. Most magnetic materials are therefore alloys or oxides of these elements or contain them in another form. There is, however, recent and increased research into new magnetic materials such as plastic magnets (organic polymers), molecular magnets (often still based on transition metals) or molecule based magnets (in which magnetism arises from strongly localized s and p electrons).

Electrodynamics gives us a first impression of magnetism. Magnetic fields act on moving electric charges or, in other words, currents. Very roughly one may understand the behavior of materials in magnetic fields as arising from the presence of "moving charges". (Bound) core and/or (quasi-free) valence electrons possess a spin, which in a simplified classical picture can be viewed as a rotating charge, i.e. a current. Bound electrons have an additional orbital momentum, which adds another source of current (again in a simplistic classical picture). These "microscopic currents" react in two different ways to an applied magnetic field: First, according to Lenz' law a current is induced that creates a magnetic field opposing the external magnetic field (diamagnetism). Second, the "individual magnets" represented by the electron currents align with the external field and enhance it (paramagnetism). If these effects happen for each "individual magnet" independently, they remain small. The corresponding magnetic properties of the material may then be understood from the individual behavior of the constituents, i.e. atoms/ions (insulators, semiconductors) or atoms/ions and free electrons (conductors), cf. section 8.3. The much stronger ferromagnetism, on the other hand, arises from a collective behavior of the "individual magnets" in the material. In section 8.4 we will first discuss the source for such an interaction, before we move on to simple models treating either a possible coupling of localized moments or itinerant ferromagnetism.

8.2 Macroscopic Electrodynamics

Before we plunge into the microscopic sources of magnetism in solids, let us first recap a few definitions from macroscopic electrodynamics. In vacuum we have $\mathbf{E}$ and $\mathbf{B}$ as the electric field (unit: V/m) and the magnetic flux density (unit: Tesla = $\mathrm{Vs/m^2}$), respectively. Note that both are vector quantities, and in principle they are also functions of space and time. Since we will only deal with constant, uniform fields in this lecture, this dependence will be dropped throughout. Inside macroscopic media, both fields can be affected by the charges and currents present in the material, yielding the two new net fields, $\mathbf{D}$ (electric displacement, unit: $\mathrm{As/m^2}$) and $\mathbf{H}$ (magnetic field, unit: A/m). For the formulation of macroscopic electrodynamics (the Maxwell equations in particular) we therefore need so-called *constitutive relations* between the external (applied) and internal (effective) fields:

$$\mathbf{D} = \mathbf{D}(\mathbf{E}, \mathbf{B}), \qquad \mathbf{H} = \mathbf{H}(\mathbf{E}, \mathbf{B}). \tag{8.1}$$

In general, this functional dependence can be written in form of a multipole expansion. In most materials, however, already the first (dipole) contribution is sufficient. These dipole terms are called $\mathbf{P}$ (el. polarization) and $\mathbf{M}$ (magnetization), and we can write

$$\mathbf{H} = (1/\mu_o)\mathbf{B} - \mathbf{M} + \ldots \tag{8.2}$$

$$\mathbf{D} = \epsilon_o \mathbf{E} + \mathbf{P} + \ldots, \tag{8.3}$$

where $\epsilon_o = 8.85 \cdot 10^{-12}\,\mathrm{As/Vm}$ and $\mu_o = 4\pi \cdot 10^{-7}\,\mathrm{Vs/Am}$ are the dielectric constant and permeability of vacuum, respectively. $\mathbf{P}$ and $\mathbf{M}$ depend on the applied field, which we can formally write as a Taylor expansion in $\mathbf{E}$ and $\mathbf{B}$. If the applied fields are not too strong, one can truncate this series after the first term (linear response), i.e. the induced polarization/magnetization is then simply proportional to the applied field. We will see below that external magnetic fields we can generate at present in the laboratory are indeed weak compared to microscopic magnetic fields, i.e. the assumption of a magnetic linear response is often well justified. As a side note, current high-intensity lasers may, however, bring us easily out of the linear response regime for the electric polarization. Corresponding phenomena are treated in the field of non-linear optics.
For the magnetization it is actually more convenient to expand in the internal field $\mathbf{H}$ instead of in $\mathbf{B}$. In the linear response regime, we thus obtain for the induced magnetization and the electric polarization

$$\mathbf{M} = (1/\mu_o)\, \chi^{\mathrm{mag}}\, \mathbf{H} \tag{8.4}$$

$$\mathbf{P} = \epsilon_o\, \chi\, \mathbf{E}, \tag{8.5}$$

where $\chi^{\mathrm{el/mag}}$ is the dimensionless electric/magnetic susceptibility tensor. In simple materials (on which we will focus in this lecture), the linear response is often isotropic in space and parallel to the applied field. The susceptibility tensors then reduce to scalar form and we can simplify to

$$\mathbf{M} = (1/\mu_o)\chi^{\mathrm{mag}}\, \mathbf{H} \tag{8.6}$$

$$\mathbf{P} = \epsilon_o \chi^{\mathrm{el}}\, \mathbf{E}. \tag{8.7}$$

These equations are in fact often directly written as defining equations for the dimensionless susceptibility *constants* in solid state textbooks. It is important to remember, however,

material	susceptibility $\chi^{\rm mag}$	
vacuum	0	
H_20	-8·10^{-6}	diamagnetic
Cu	$\sim$ -10^{-5}	diamagnetic
Al	2·10^{-5}	paramagnetic
iron (depends on purity)	$\sim$ 100 - 1000	ferromagnetic
μ-metal (nickle-iron alloy)	$\sim$ 80,000 - 100,000	basically screens everything (used in magnetic shielding)

Table 8.1: Magnetic susceptibility of some materials.

that we made the dipole approximation and restricted ourselves to isotropic media. For this case, the constitutive relations between external and internal field reduce to

$$\mathbf{H} = \frac{1}{\mu_o \mu_r}\,\mathbf{B} \tag{8.8}$$

$$\mathbf{D} = \epsilon_o \epsilon_r\,\mathbf{E}, \tag{8.9}$$

where $\epsilon_r = 1 + \chi^{\rm el}$ is the relative dielectric constant, and $\mu_r = 1 - \chi^{\rm mag}$ the relative permeability of the medium. For $\chi^{\rm mag} < 0$, we have $\mu < 1$ and $|\mathbf{H}| < |\frac{1}{\mu_0}\mathbf{B}|$. The response of the medium reduces (or in other words *screens*) the external field. Such a system is called *diamagnetic*. For the opposite case ($\chi^{\rm mag} > 0$) we have $\mu > 1$ and therefore $|\mathbf{H}| > |\frac{1}{\mu_0}\mathbf{B}|$. The external field is enhanced by the material, and we talk about *paramagnetism*.
To connect to microscopic theories we consider the energy. The process of screening or enhancing the external field will require work, i.e. the energy of the system is changed (magnetic energy). Assume therefore that we have a material of volume V, which we bring into a magnetic field B (which for simplicity we take to be along one dimension only). From electrodynamics we know that the energy of this magnetic field is

$$E^{\rm mag} = (1/2BH)V \qquad \Rightarrow \quad 1/V dE^{\rm mag} = 1/2BdH + 1/2HdB. \tag{8.10}$$

From eq. (8.9) we find $dB = \mu_o\mu_r dH$ and therefore $HdB = BdH$, which leads to

$$1/V dE^{\rm mag} = BdH = (\mu_o H + \mu_o M)dH = B_o dH + \mu_o M dH. \tag{8.11}$$

In the first term, we have realized that $\mu_o H = B_o$ is just the field in the vacuum, i.e. without the material. This term therefore gives the field induced energy change, if no material was present. Only the second term is material dependent and describes the energy change of the material in reaction to the applied field. The energy change of the material itself is therefore

$$dE^{\rm mag}_{\rm material} = -\mu_o M V dH. \tag{8.12}$$

Recalling that the energy of a dipole with magnetic moment m in a magnetic field is $E = -mB$, we see that the approximations leading to eq. (8.9) mean nothing else but assuming that the homogeneous solid is build up of a constant density of "molecular dipoles", i.e. the magnetization M is the (average) dipole moment density.
Rearranging eq. (8.12), we arrive finally at an expression that is a special case of a frequently employed alternative *definition* of the magnetization

$$M(H) = -\frac{1}{\mu_o V}\left.\frac{\partial E(H)}{\partial H}\right|_{S,V}, \tag{8.13}$$

and in turn of the susceptibility

$$\chi^{\rm mag}(H) \;=\; \left.\frac{\partial M(H)}{\partial H}\right|_{S,V} \;=\; -\frac{1}{\mu_o V}\;\left.\frac{\partial^2 E(H)}{\partial H^2}\right|_{S,V}. \tag{8.14}$$

At finite temperatures, it is straightforward to generalize these definitions to

$$M(H,T) = -\frac{1}{\mu_o V}\;\left.\frac{\partial F(H,T)}{\partial H}\right|_{S,V} \qquad \chi^{\rm mag}(H,T) = -\frac{1}{\mu_o V}\;\left.\frac{\partial^2 F(H,T)}{\partial H^2}\right|_{S,V}. \tag{8.15}$$

While the derivation via macroscopic electrodynamics is most illustrative, we will see that these last two equations will be much more useful for the actual quantum-mechanical computation of the magnetization and susceptibility of real systems. All we have to do, is to derive an expression for the energy of the system as a function of the applied external field. The first and second derivatives with respect to the field then yield M and $\chi^{\rm mag}$, respectively.

8.3 Magnetism of atoms and free electrons

We had already discussed that magnetism arises from the "microscopic currents" connected to the orbital and spin moments of electrons. Each electron therefore represents a "microscopic magnet", but how do they couple in materials, with a large number of electrons? Since any material is composed of atoms it is reasonable to first reduce the problem to that of the electronic coupling inside an atom, before attempting to describe the coupling of "atomic magnets". Since both orbital and spin momentum of all bound electrons of an atom will contribute to its magnetic behavior, it will be useful to first recall how the total electronic angular momentum of an atom is determined (section 8.3.1), before we turn to the effect of a magnetic field on the atomic Hamiltonian (section 8.3.2). In metals, we have the additional presence of free conduction electrons, the magnetism of which will be addressed in section 8.3.3. Finally, we will discuss in section 8.3.4, which aspects of magnetism we can already understand just on the basis of these results on atomic magnetism, i.e. in the limit of vanishing coupling between the "atomic magnets".

8.3.1 Total angular momentum of atoms

In the atomic shell model, the possible quantum states of electrons are labeled as nlm_l, where n is the *principle quantum number*, l the *orbital quantum number*, and m_l the *orbital magnetic quantum number*. For any given n, defining a so-called "shell", the orbital quantum number l can take only integer values between 0 and $(n-1)$. For $l = 0, 1, 2, 3\ldots$, we generally use the letters s, p, d, f and so on. Within such an nl "subshell", the orbital magnetic number m_l may have the $(2l+1)$ integer values between $-l$ and $+l$. The last quantum number, the spin magnetic quantum number m_s, takes the values $-1/2$ and $+1/2$. For the example of the first two shells this leads to two $1s$, two $2s$, and six $2p$ states.

When an atom has more than one electron, the *Pauli exclusion principle* dictates that each quantum state specified by the set of four quantum numbers nlm_lm_s can only be occupied by one electron. In all but the heaviest ions, spin-orbit coupling[1] is negligible. In

[1]Spin-orbit (or LS) coupling is a relativistic effect that requires the solution of the Dirac equation.

this case, the Hamiltonian does not depend on spin or the orbital moment and therefore commutes with these quantum numbers (Russel-Saunders coupling). The total orbital and spin angular momentum for a given subshell are then good quantum numbers and are given by

$$L = \sum m_l \qquad \text{and} \qquad S = \sum m_s. \tag{8.16}$$

If a subshell is completely filled, it is easy to verify that L=S=0. The total electronic angular momentum of an atom $J = L + S$, is therefore determined by the partially filled subshells. The occupation of quantum states in a partially filled shell is given by Hund's rules:

1. The states are occupied so that as many electrons as possible (within the limitations of the Pauli exclusion principle) have their spins aligned parallel to one another, i.e., so that the value of S is as large as possible.

2. When determined how the spins are assigned, then the electrons occupy states such that the value of L is a maximum.

3. The total angular momentum J is obtained by combining L and S as follows:

   - if the subshell is less than half filled (i.e., if the number of electrons is $< 2l+1$), then $J = L - S$;
   - if the subshell is more than half filled (i.e., if the number of electrons is $> 2l+1$), then $J = L + S$;
   - if the subshell is exactly half filled (i.e., if the number of electrons is $= 2l + 1$), then $L = 0, J = S$.

The first two Hund's rules are determined purely from electrostatic energy considerations (e.g. electrons with equal spins are farther away from each other on account of the exchange-hole). Only the third rule follows from spin-orbit coupling. Each quantum state in this partially filled subshell is called a *multiplet*. The term comes from the spectroscopy community and refers to multiple lines (peaks) that have the same origin (in this case the same subshell nl). Without any interaction (e.g. electron-electron, spin-orbit, etc.) all quantum states in this subshell would be energetically degenerate and the spectrum would show only one peak at this energy. The interaction lifts the degeneracy and in an ensemble of atoms different atoms might be in different quantum states. The single peak then splits into multiple peaks in the spectrum. The notation for the *ground-state multiplet*, obtained by Hund's rules is not simply denoted LSJ as one would have expected. Instead, for historical reasons, the notation ${}^{(2S+1)}L_J$ is used. To make matters worse, the angular momentum symbols are used for the total angular momentum ($L = 0, 1, 2, 3, \ldots = S, P, D, F, \ldots$). The rules are in fact easier to apply than their description might suggest at first glance. Table 8.2 lists the filling and notation for the example of a d-shell.

8.3.2 General derivation of atomic susceptibilities

Having determined the total angular momentum of an atom, we now turn to the effect of a uniform magnetic field $\mathbf{H}$ (taken along the z-axis) on the electronic Hamiltonian of an atom $H^e = T^e + V^{e-ion} + V^{e-e}$. Note that the focus on H^e means that we neglect the

el.	$m_l =$	2	1	0	−1	−2	S	$L = \lvert\sum m_l\rvert$	J	Symbol
1		↓					1/2	2	3/2	$^2D_{3/2}$
2		↓	↓				1	3	2	$^3F_2$
3		↓	↓	↓			3/2	3	3/2	$^4F_{3/2}$
4		↓	↓	↓	↓		2	2	0	$^5D_0$
5		↓	↓	↓	↓	↓	5/2	0	5/2	$^6S_{5/2}$
6		↓↑	↓	↓	↓	↓	2	2	4	$^5D_4$
7		↓↑	↓↑	↓	↓	↓	3/2	3	9/2	$^4F_{9/2}$
8		↓↑	↓↑	↓↑	↓	↓	1	3	4	$^3F_4$
9		↓↑	↓↑	↓↑	↓↑	↓	1/2	2	5/2	$^2D_{5/2}$
10		↓↑	↓↑	↓↑	↓↑	↓↑	0	0	0	$^1S_0$

Table 8.2: Ground states of ions with partially filled d-shells ($l = 2$), as constructed from Hund's rules.

effect of $\mathbf{H}$ on the nuclear motion and spin. This is in general justified by the much greater mass of the nuclei (rendering the nuclear contribution to the atomic magnetic moment very small), but it would of course be crucial if we were to address e.g. nuclear magnetic resonance (NMR) experiments. Since V^{e-ion} and V^{e-e} are not affected by the magnetic field, we are left with the kinetic energy operator.
From classical electrodynamics we know that in the presence of a magnetic field, we have to replace all momenta $\mathbf{p}$ ($= i\hbar\nabla$) by the canonic momenta $\mathbf{p} \to \mathbf{p} + e\mathbf{A}$. For a uniform magnetic field (along the z-axis), a suitable vector potential $\mathbf{A}$ is

$$\mathbf{A} = -\frac{1}{2}\left(\mathbf{r} \times \mu_0\mathbf{H}\right), \tag{8.17}$$

for which it is straightforward to verify that it fulfills the conditions $\mathbf{H} = (\nabla \times \mathbf{A})$ and $\nabla \cdot \mathbf{A} = 0$. The total kinetic energy operator is then written

$$T^e(\mathbf{H}) = \frac{1}{2m}\sum_k \left[\mathbf{p}_k + e\mathbf{A}\right]^2 = \frac{1}{2m}\sum_k \left[\mathbf{p}_k - \frac{e}{2}\left(\mathbf{r}_k \times \mu_0\mathbf{H}\right)\right]^2 \quad . \tag{8.18}$$

Expanding the square leads to

$$\begin{aligned} T^e(\mathbf{B}) &= \sum_k \left[\frac{p_k^2}{2m} + \frac{e}{2m}\mathbf{p}_k \cdot (\mu_0\mathbf{H} \times \mathbf{r}_k) + \frac{e^2}{8m}\left(\mathbf{r}_k \times \mu_0\mathbf{H}\right)^2\right] \\ &= T_o^e + \sum_k \frac{e}{2m}\left(\mathbf{r}_k \times \mathbf{p}_k\right) \cdot \mu_0\mathbf{H} + \frac{e^2\mu_0^2}{8m}H^2\sum_k \left(x_k^2 + y_k^2\right) \quad , \end{aligned} \tag{8.19}$$

where we have used the fact that $\mathbf{p} \cdot \mathbf{A} = \mathbf{A} \cdot \mathbf{p}$, if $\nabla\mathbf{A} = 0$. If we exploit that the total electronic orbital momentum operator $\mathbf{L}$ can be expressed as $\hbar\mathbf{L} = \sum_k (\mathbf{r}_k \times \mathbf{p}_k)$, and introduce the Bohr magneton $\mu_B = (e\hbar/2m) = 0.579 \cdot 10^{-4}\,\mathrm{eV/T}$, the variation of the kinetic energy operator due to the magnetic field can be further simplified to

$$\Delta T^e(\mathbf{B}) = \mu_B\mu_0\mathbf{L} \cdot \mathbf{H} + \frac{e^2\mu_0}{8m}H^2\sum_k \left(x_k^2 + y_k^2\right) \quad . \tag{8.20}$$

If this was the only effect of the magnetic field on H^e, one can, however, show that the magnetization in thermal equilibrium must always vanish (Bohr-van Leeuwen theorem). In simple terms this is, because the vector potential amounts to a simple shift in $\mathbf{p}$, which integrates out, when summed over all momenta. The free energy is then independent of $\mathbf{H}$ and the magnetization is zero.
However, in reality the magnetization does not vanish. The problem is that we have used the wrong kinetic energy operator. We should have solved the relativistic Dirac equation

$$\begin{pmatrix} V & c\sigma\mathbf{p} \\ c\sigma\mathbf{p} & -2c^2+V \end{pmatrix} \begin{pmatrix} \phi \\ \chi \end{pmatrix} = E \begin{pmatrix} \phi \\ \chi \end{pmatrix} \tag{8.21}$$

where $\phi = \begin{pmatrix} \phi_\uparrow \\ \phi_\downarrow \end{pmatrix}$ is an electron wave function and $\chi = \begin{pmatrix} \chi_\uparrow \\ \chi_\downarrow \end{pmatrix}$ a positron one. σ is a vector of 2×2 Pauli spin matrices. We should have introduced the vector potential in the Dirac equation, but to fully understand the electron-field interaction one would have to resort to quantum electro dynamics (QED), which goes far beyond the scope of this lecture.
We therefore heuristically introduce another momentum, the electron spin, that emerges from the full relativistic treatment.The new interaction energy term has the form

$$\Delta H^{\rm spin}(\mathbf{H}) = g_0 \mu_B \mu_0 \mathbf{H}\mathbf{S}_z\,, \quad \text{where} \quad \mathbf{S}_z = \sum_k \mathbf{s}_{z,k} \quad . \tag{8.22}$$

Here g_0 is the so-called electronic *g-factor* (i.e., the g-factor for one electron spin). In the Dirac equation $g_0 = 2$, whereas in QED one obtains

$$\begin{aligned} g_0 &= 2\left[1 + \frac{\alpha}{2\pi} + O(\alpha^2) + \ldots\right], \quad \text{where} \quad \alpha = \frac{e^2}{\hbar c} \approx \frac{1}{137} \quad , \\ &= 2.0023\ldots, \end{aligned} \tag{8.23}$$

which we usually take as just 2.
The total field-dependent Hamiltonian is therefore,

$$\Delta H^e(\mathbf{H}) = \Delta T^e(\mathbf{H}) + \Delta H^{\rm spin}(\mathbf{H}) \;=\; \mu_0\mu_B\,(\mathbf{L} + g_0\mathbf{S})\cdot\mathbf{H} + \frac{e^2\mu_0^2}{8m} H^2 \sum_k \left(x_k^2 + y_k^2\right). \tag{8.24}$$

We will see below that the energy shifts produced by eq. (8.24) are generally quite small on the scale of atomic excitation energies, even for the highest presently attainable laboratory field strengths. Perturbation theory can thus be used to calculate the changes in the energies connected with this modified Hamiltonian. Remember that magnetization and susceptibility were the first and second derivative of the field-dependent energy with respect to the field, which is why we would like to write the energy as a function of $\mathbf{H}$. Since we lateron we require the second derivative, terms to second order in $\mathbf{H}$ must be retained. Recalling second order perturbation theory, we can write the energy of the nth *non-degenerate* level of the unperturbed Hamiltonian as

$$E_n \to E_n + \Delta E_n(\mathbf{H}); \quad \Delta E_n = <n|\Delta H^e(\mathbf{H})|n> + \sum_{n'\neq n} \frac{|<n|\Delta H^e(\mathbf{H})|n'>|^2}{E_n - E_n'} \quad . \tag{8.25}$$

Substituting eq. (8.24) into the above, and retaining terms to quadratic order in $\mathbf{H}$, we arrive at the basic equation for the theory of the magnetic susceptibility of atoms:

$$\begin{aligned}\Delta E_n &= \mu_B \mathbf{B}\cdot < n|\mathbf{L} + g_0\mathbf{S}|n > + \frac{e^2}{8m}B^2 < n|\sum_k \left(x_k^2 + y_k^2\right)|n > \\ &+ \sum_{n'\neq n} \frac{|< n|\mu_B \mathbf{B}\cdot(\mathbf{L} + g_0\mathbf{S})|n' > |^2}{E_n - E_{n'}} \quad . \end{aligned} \tag{8.26}$$

Since we are mostly interested in the atomic ground state $|0>$, we will now proceed to evaluate the magnitude of the three terms contained in eq. (8.26) and their corresponding susceptibilities. This will also give us a feeling of the physics behind the different contributions.

8.3.2.1 Second term: Larmor/Langevin diamagnetism

To obtain an estimate for the magnitude of this term, we assume spherically symmetric wavefunctions ($< 0|\sum_k (x_k^2 + y_k^2)|0 > \approx 2/3 < 0|\sum_k r_k^2|0 >$). This allows us to approximate the energy shift in the atomic ground state due to the second term as

$$\Delta E_0^{\rm dia} \approx \frac{e^2\mu_0^2 H^2}{12m}\sum_k < 0|r_k^2|0 > \sim \frac{e^2\mu_0 H^2}{12m} Z\,\bar{r}^2_{\rm atom} \quad , \tag{8.27}$$

where Z is the total number of electrons in the atom (resulting from the sum over the k electrons in the atom), and $\bar{r}^2_{\rm atom}$ is the mean square atomic radius. If we take $Z \sim 30$ and $\bar{r}^2_{\rm atom}$ of the order of Å^2, we find $\Delta E_0^{\rm dia} \sim 10^{-9}$ eV even for fields of the order of Tesla. This contribution is therefore rather small. We make a similar observation from an order of magnitude estimate for the susceptibility,

$$\chi^{\rm mag,dia} = -\frac{1}{\mu_0 V}\frac{\partial^2 E_0}{\partial H^2} = -\frac{\mu_0 e^2 Z \bar{r}^2_{\rm atom}}{6mV} \sim -10^{-4}. \tag{8.28}$$

With $\chi^{\rm mag,dia} < 0$, this term represents a diamagnetic contribution (so-called Larmor or Langevin diamagnetism), i.e. the associated magnetic moment screens the external field. We have thus identified the term which we qualitatively expected to arise out of the induction currents initiated by the applied magnetic field.

We will see below that this diamagnetic contribution will only determine the overall magnetic susceptibility of the atom, when the other two terms in eq. (8.26) vanish. This is only the case for atoms with $\mathbf{J}|0 >= \mathbf{L}|0 >= \mathbf{S}|0 >$, i.e. for closed shell atoms or ions (e.g. the noble gas atoms). In this case, the ground state $|0>$ is indeed non-degenerate, which justified our use of eq. (8.26) to calculate the energy level shift, and from chapter 6 on cohesion we recall that the first excited state is much higher in energy. In all but the highest temperatures, there is then also a negligible probability of the atom being in any but its ground state in thermal equilibrium. This means that the diamagnetic susceptibility will be largely temperature independent (otherwise it would have been necessary to use eq. (8.15) for the derivation of $\chi^{\rm mag,dia}$).

8.3.2.2 Third term: Van Vleck paramagnetism

By taking the second derivative of the third term in eq. (8.26), we obtain for its susceptibility

$$\chi^{\rm mag,vleck} \;=\; \frac{2\mu_o\mu_B^2}{V}\sum_n \frac{|<0|(\mathbf{L_z}+g_0\mathbf{S_z})|n>|^2}{E_n-E_0}. \tag{8.29}$$

Note that we have reversed the order in the denominator as compared to eq. (8.26), which compensates the minus sign in the definition of the susceptibility in eq. (8.14). Since the energy of any excited state will necessarily be higher than the ground state energy ($E_n > E_0$), $\chi^{\rm mag,vleck} > 0$. The third term therefore represents a paramagnetic contribution (so-called Van Vleck paramagnetism), which is connected to field-induced electronic transitions. If the electronic ground state is non-degenerate (and only for this case, does the above formula hold), it is precisely the normally quite large separation between electronic states which makes this term similarly small as the diamagnetic one. Van Vleck paramagnetism therefore only plays a role for atoms or ions with shells that are one electron short of being half filled (which is the only case when the third term in eq. (8.26) does not vanish, while the first term does). The magnetic behavior of such atoms or ions is determined by a balance between Larmor diamagnetism and Van Vleck paramagnetism. Both terms are small, and tend to cancel each other. The atomic lanthanide series is a notable exception. In Sm and Eu the energy spacing between the ground and excited states is small enough so that Van Vleck paramagnetism prevails and dominates (see Fig. 8.2). Here the effective magneton number μ_{eff} is plotted, which is defined in terms of the susceptibility $\chi = \frac{N\mu_{eff}^2\mu_B^2}{3k_BT}$.

8.3.2.3 First term: Paramagnetism

For any atom with $J \neq 0$ (which is the case for most atoms), the first term does not vanish and will then completely dominate the magnetic behavior. Anticipating this result, we will neglect the second and third term in eq. (8.26) for the moment. Atoms with $J \neq 0$ have a $(2J+1)$-fold degenerate ground state, which implies that the simple form of eq. (8.26) can not be applied. Instead, the $\alpha = 1, \ldots, (2J+1)$ energy shifts within the ground state subspace are given by

$$\Delta E_{0,\alpha} \;=\; \mu_B B \sum_{\alpha'=1}^{(2J+1)} <0\alpha|\mathbf{L_z}+g_0\mathbf{S_z}|0\alpha'> = \;\mu_B B \sum_{\alpha'=1}^{(2J+1)} V_{\alpha,\alpha'}, \tag{8.30}$$

where we have again aligned the magnetic field with the z-axis, and have defined the interaction matrix $V_{\alpha,\alpha'}$. The energy shifts are then obtained by diagonalizing the interaction matrix within the ground state subspace. This is a standard problem in atomic physics (see e.g. Ashcroft/Mermin), and one finds that the basis diagonalizing this matrix are the states of defined J and J_z,

$$< JLS, J_z|\mathbf{L_z}+g_0\mathbf{S_z}|JLS, J_z'> = \; g(JLS)J_z\;\delta_{J_z,J_{z'}}. \tag{8.31}$$

where JLS are the quantum numbers defining the atomic ground state $|0>$ in the shell model, and $g(JLS)$ is the so-called *Landé g-factor*. Setting $g_o \approx 2$, this factor is obtained as

$$g(JLS) \;=\; \frac{3}{2} \;+\; \frac{1}{2}\left[\frac{S(S+1)-L(L+1)}{J(J+1)}\right] \quad . \tag{8.32}$$

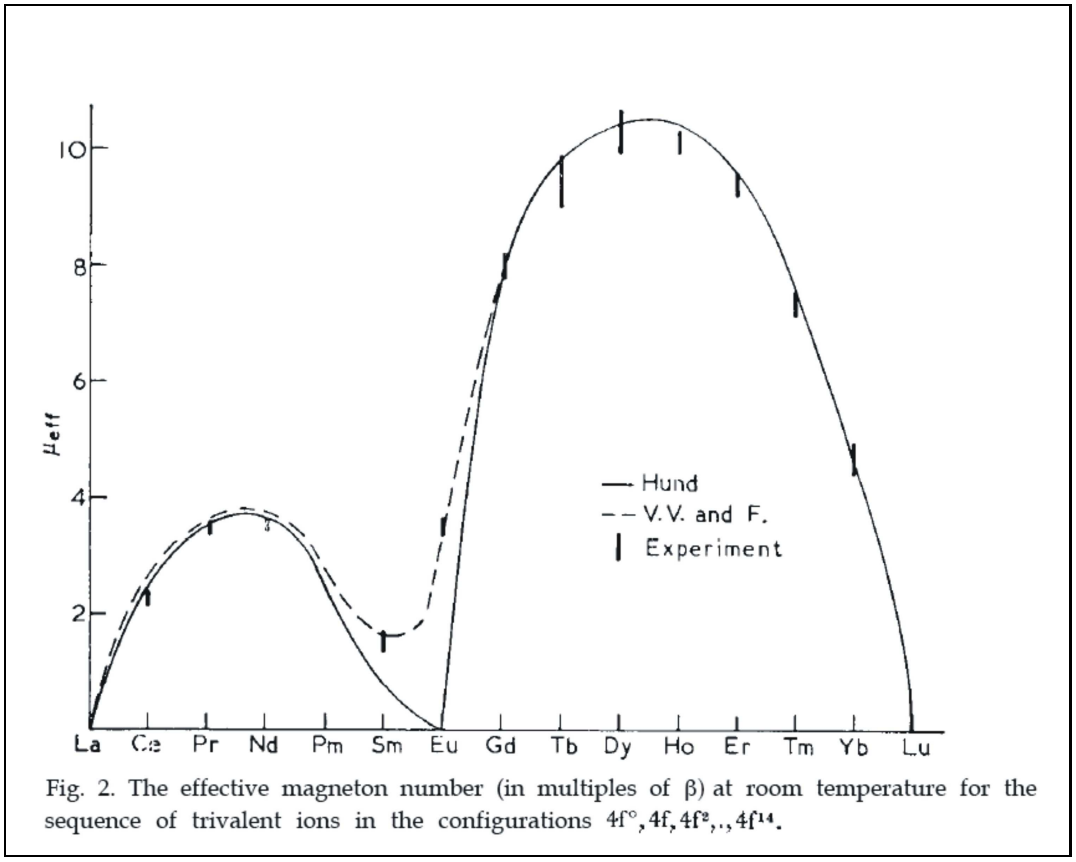

Fig. 2. The effective magneton number (in multiples of β) at room temperature for the sequence of trivalent ions in the configurations $4f^{\circ}, 4f, 4f^{2}, ., 4f^{14}$.

Figure 8.2: Van Vleck paramagnetism for Sm and Eu in the lanthanide atoms. From Van Vleck's nobel lecture.

If we insert eq. (8.31) into eq. (8.30), we obtain

$$\Delta E_{JLS,J_z} \;=\; g(JLS)\mu_B J_z\, B \quad , \tag{8.33}$$

i.e. the magnetic field splits the degenerate ground state into $(2J+1)$ equidistant levels separated by $g(JLS)\mu_B B$ (i.e. $-g(JLS)\mu_B JB, -g(JLS)\mu_B(J-1)B, \ldots, +g(JLS)\mu_B(J-1)B, +g(JLS)\mu_B JB$). This is the same effect, as the magnetic field would have on a magnetic dipole with magnetic moment

$$\mathbf{m}_{\text{atom}} = -g(JLS)\mu_B\, \mathbf{J}. \tag{8.34}$$

The first term in eq. (8.26) can therefore be interpreted as the expected paramagnetic contribution due to the alignment of a "microscopic magnet". This is of course only true when we have unpaired electrons in partially filled shells of the atom ($J \neq 0$).
Before we proceed to derive the paramagnetic susceptibility that arises from this contribution, we note that this identification of $\mathbf{m}_{\text{atom}}$ via eq. (8.26) serves nicely to illustrate the difference between phenomenological and so-called first-principles theories. We have seen that the simple Hamiltonian $H^{\text{spin}} = -\mu_0 \mathbf{m}_{\text{atom}} \cdot \mathbf{H}$ would equally well describe the splitting of the $(2J+1)$ ground state levels. If we had only known this splitting, e.g. from experiment (*Zeeman effect*), we could have simply used H^{spin} as a phenomenological, so-called "spin Hamiltonian". By fitting to the experimental splitting, we could even have obtained the magnitude of the magnetic moment for individual atoms (which due to their different total angular momenta is of course different for different species). Examining the fitted magnitudes, we might even have discovered that the splitting is connected to the total angular momentum. The virtue of the first-principles derivation used in this lecture, on the other hand, is that this prefactor is directly obtained, without any fitting to experimental data. This allows us not only to unambiguously check our theory by comparison with the experimental data (which is not possible in the phenomenological theory, where the fitting can often easily cover up for deficiencies in the assumed ansatz). We also directly obtain the dependence on the total angular momentum, and can even predict the properties of atoms which have not (yet) been measured. Admittedly, in many cases first-principles theories are harder to derive. Later we will see more examples of "spin Hamiltonians", which describe the observed magnetic behavior of the material very well, but an all-encompassing first-principles theory is still lacking.

8.3.2.4 Paramagnetic susceptibility: Curie's law

The separation of the $(2J+1)$ ground state levels of a paramagnetic atom in a magnetic field is $g(JLS)\mu_0\mu_B H$. Recalling that $\mu_B = 0.579 \cdot 10^{-4}\,\text{eV/T}$, we see that the splitting is only of the order of $10^{-4}\,\text{eV}$, even for fields of the order of Tesla. This is small compared to $k_B T$ for realistic temperatures. At finite temperature, more than one level will therefore be populated and we have to use statistical mechanics to evaluate the free energy. The magnetization then follows from eq. (8.15). The Helmholtz free energy

$$F = -k_B T \ln Z \tag{8.35}$$

is given in terms of the partition function Z with

$$Z = \sum_n e^{-\frac{E_n}{k_B T}}. \tag{8.36}$$

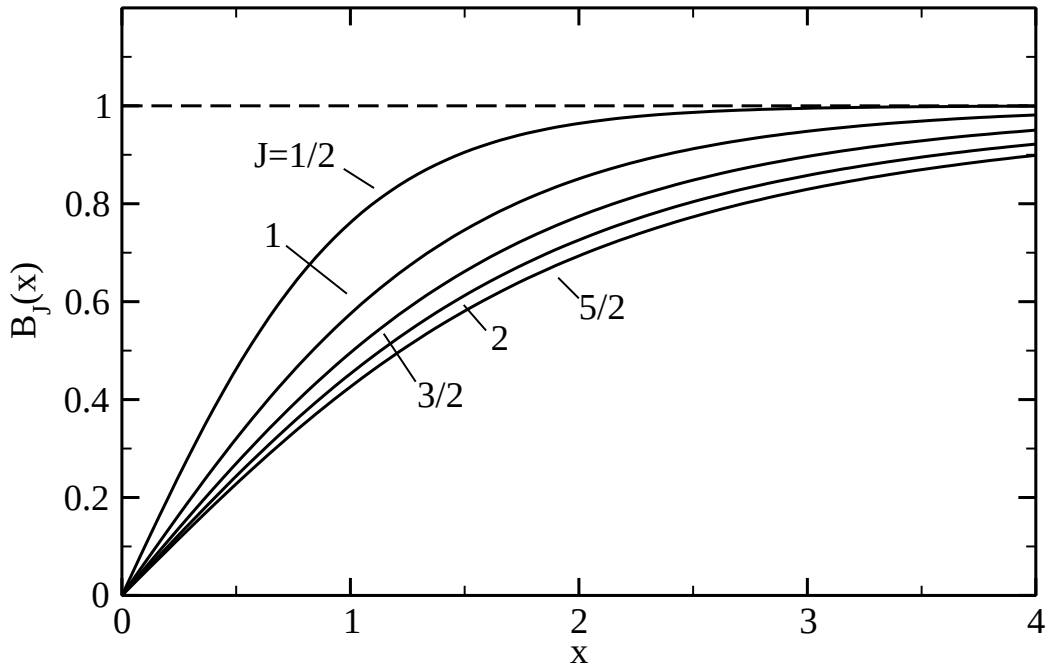

Figure 8.3: Plot of the Brillouin function $B_J(x)$ for various values of the spin J (the total angular momentum).

Here n is $J_z = -J, \ldots, J$ and E_n is our energy spacing $g(JLS)\mu_0\mu_B H J_z$. Defining $\eta = g(JLS)\mu_B B)/(k_B T)$ (i.e. the fraction of magnetic versus thermal energy), the partition function becomes

$$\begin{aligned} Z &= \sum_{J_z=-J}^{J} e^{-\eta J_z} = \frac{e^{-\eta J} - e^{\eta(J+1)}}{1 - e^{\eta}} \\ &= \frac{e^{-\eta(J+1/2)} - e^{\eta(J+1/2)}}{e^{-\eta/2} - e^{\eta/2}} = \frac{\sinh\left[(J+1/2)\eta\right]}{\sinh\left[\eta/2\right]} \quad . \end{aligned} \tag{8.37}$$

With this, one finds for the magnetization

$$\begin{aligned} M(T) &= -\frac{1}{\mu_0 V}\frac{\partial F}{\partial H} = -\frac{1}{\mu_0 V}\frac{\partial(-k_B T \ln Z)}{\partial H} \\ &= \frac{k_B T}{\mu_0 V}\frac{\partial}{\partial H}\left[\ln\left(\sinh[(J+1/2)\eta]\right) - \ln\left(\sinh[\eta/2]\right)\right] = \frac{g(JLS)\mu_B J}{V} B_J(\eta), \end{aligned} \tag{8.38}$$

where in the last step, we have defined the so-called *Brillouin function*

$$B_J(\eta) = \frac{1}{J}\left\{(J+\frac{1}{2})\coth\left[(J+\frac{1}{2})\eta/J\right] - \frac{1}{2}\coth\left[\frac{\eta}{2J}\right]\right\} \quad . \tag{8.39}$$

As shown in Fig. 8.3, $B_J \to 1$ for $\eta \gg 1$, in which case eq. (8.38) simply tells us that all atomic magnets with momentum $\mathbf{m}_{\rm atom}$, cf. eq. (8.34), have aligned to the external field, and the magnetization reaches its maximum value of $M = m_{\rm atom}/V$, i.e. the magnetic moment density.

We had, however, discussed above, that $\eta = (g(JLS)\mu_B B)/(k_B T)$ will be much smaller than unity for normal field strengths. At all but the lowest temperatures, the other limit for the Brillouin function, i.e. $B_J(\eta \to 0)$, will therefore be much more relevant. This small η-expansion is

$$B_J(\eta \ll 1) \approx \frac{J+1}{3}\eta + O(\eta^3) \quad . \tag{8.40}$$

In this limit, we finally obtain for the paramagnetic susceptibility

$$\chi^{\text{mag,para}}(T) = \frac{\partial M}{\partial H} = \frac{\mu_o \mu_B^2 g(JLS)^2 J(J+1)}{3Vk_B}\frac{1}{T} = \frac{C}{T} \quad . \tag{8.41}$$

With $\chi^{\text{mag,para}} > 0$, we have now confirmed our previous hypothesis, that the first term in eq. (8.26) gives a paramagnetic contribution. The inverse dependence of the susceptibility on temperature is known as *Curie's law*, $\chi^{\text{mag,para}} = C_{\text{Curie}}/T$ with C_{Curie} the Curie constant. Such a dependence is characteristic for a system with "molecular magnets" whose alignment is favored by the applied field, and that is opposed by thermal disorder. Again, we see that the first-principles derivation allows not only shows us the validity range of this empirical law (remember that it only holds in the small η-limit), but also provides the proportionality constant in terms of fundamental properties of the system.
To make a quick size estimate, we take the volume of atomic order ($V \sim$ Å^3) to find $\chi^{\text{mag,para}} \sim 10^{-2}$ at room temperature. The paramagnetic contribution is thus orders of magnitude larger than the diamagnetic or the Van Vleck one, even at room temperature. Nevertheless, with $\chi^{\text{mag,para}} \ll 1$ it is still small compared to electric susceptibilities, which are of the order of unity. We will discuss the consequences of this in section 8.3.4, but before we have to evaluate a last remaining, additional source of magnetic behavior in metals, i.e. the free electrons.

8.3.3 Susceptibility of the free electron gas

Having determined the magnetic properties of electrons bound to ions, it is valuable to also consider the opposite extreme and examine their properties as they move nearly freely in a metal. There are again essentially two major terms in the response of free fermions to an external magnetic field. One results from the "alignment" of spins (which is a rough way of visualizing the quantum mechanical action of the field on the spins) and is called *Pauli paramagnetism*. The other arises from the orbital moments created by induced circular motions of the electrons. It thus tends to screen the exterior field and is known as *Landau diamagnetism*.
Let us first try to analyze the origin of Pauli paramagnetism and examine its order of magnitude like we have also done for all atomic magnetic effects. For this we consider again the free electron gas, i.e. N non-interacting electrons in a volume V. In chapter 2 we had already derived the density of states (DOS) per volume

$$N(\epsilon) = \frac{V}{2\pi^2}\left(\frac{2m_e}{\hbar^2}\right)^{3/2}\sqrt{\epsilon} \quad . \tag{8.42}$$

In the electronic ground state, all states are filled following the Fermi-distribution

$$\frac{N}{V} = \int_0^\infty N(\epsilon)\, f(\epsilon, T)\, d\epsilon. \tag{8.43}$$

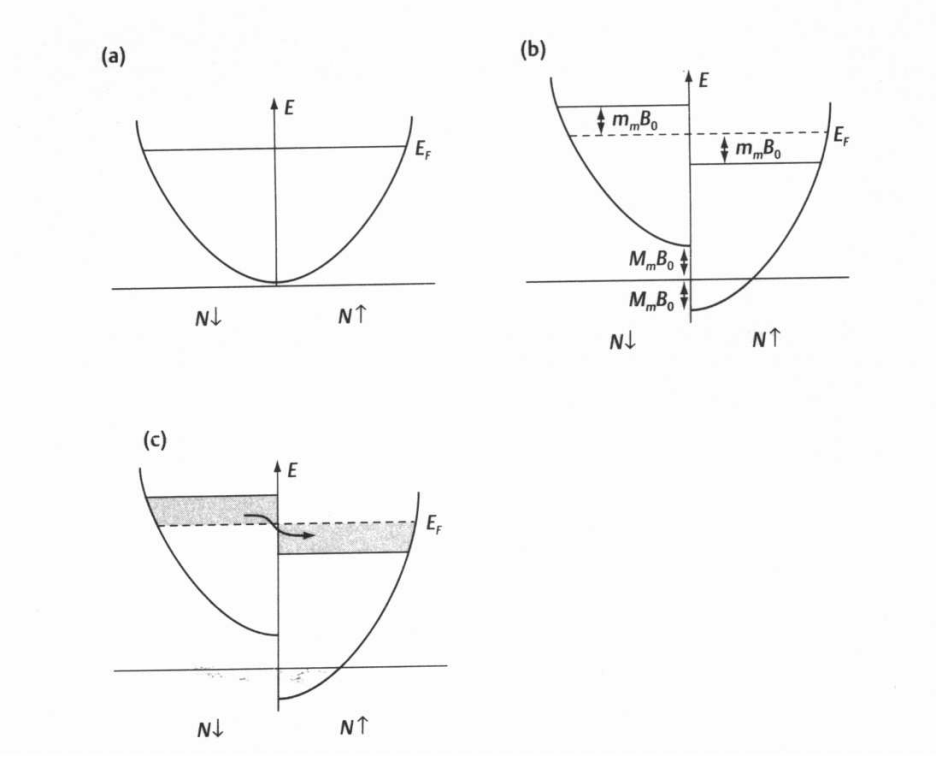

Figure 8.4: Free electron density of states and the effect of an external field: N↑ corresponds to the number of electrons with spins aligned parallel and N↓ antiparallel to the z-axis. (a) No magnetic field, (b) a magnetic field, $\mu_0\mathbf{H}_0$ is applied along the z-direction, (c) as a result of (b) some electrons with spins antiparallel to the field (shaded region on left) change their spin and move into available lower energy states with spins aligned parallel to the field.

The electron density N/V uniquely characterizes our electron gas. For sufficiently low temperatures, the Fermi-distribution can be approximated by a step function, so that all states up to the Fermi level are occupied. This Fermi level is conveniently expressed in terms of the Wigner-Seitz radius r_s that we had already defined in chapter 6

$$\epsilon_F \;=\; \frac{50.1\,\mathrm{eV}}{\left(\frac{r_s}{a_B}\right)^2} \quad . \tag{8.44}$$

The DOS at the Fermi level can then also be expressed in terms of r_s

$$N(\epsilon_F) \;=\; \left(\frac{1}{20.7\,\mathrm{eV}}\right)\left(\frac{r_s}{a_B}\right)^{-1} \quad . \tag{8.45}$$

Up to now we have not explicitly considered the spin degree of freedom, which leads to the double occupation of each electronic state with a spin up and a spin down electron. Such an explicit consideration becomes necessary, however, when we now include an external field. This is accomplished by defining spin up and spin down DOSs, $N^{\uparrow}$ and $N^{\downarrow}$, in analogy to the spin-unresolved case. In the absence of a magnetic field, the ground state of the free electron gas has an equal number of spin-up and spin-down electrons, and the

degenerate spin-DOS are therefore simply half-copies of the original total DOS defined in eq. (8.42)

$$N^{\uparrow}(\epsilon) \;=\; N^{\downarrow}(\epsilon) \;=\; \frac{1}{2}N(\epsilon) \quad , \tag{8.46}$$

cf. the graphical representation in Fig. 8.4a.
An external field $\mu_0\mathbf{H}$ will now interact differently with spin up and spin down states. Since the electron gas is fully isotropic we can always choose the spin axis that defines up and down spins to go along the direction of the applied field, and thus reduce the problem to one dimension. If we focus only on the interaction of the spin with the field and neglect the orbital response for the moment, the effect boils down to an equivalent of eq. (8.22), i.e. we have

$$\Delta H^{\text{spin}}(\mathbf{H}) \;=\; \mu_0\mu_B g_0 \mathbf{H}\cdot\mathbf{s} \;=\; +\mu_0\mu_B H \quad \text{(for spin up)} \tag{8.47}$$

$$\;=\; -\mu_0\mu_B H \quad \text{(for spin down)} \tag{8.48}$$

where we have again approximated the electronic g-factor g_0 by 2. The effect is therefore simply to shift spin up electrons relative to spin down electrons. This can be expressed via the spin DOSs

$$N^{\uparrow}(\epsilon) \;=\; \frac{1}{2}N(\epsilon - \mu_0\mu_B H) \tag{8.49}$$

$$N^{\downarrow}(\epsilon) \;=\; \frac{1}{2}N(\epsilon + \mu_0\mu_B H) \quad , \tag{8.50}$$

or again graphically by shifting the two parabolas with respect to each other as shown in Fig. 8.4b. If we now fill the electronic states according to the Fermi-distribution, a different number of up and down electrons results and our electron gas exhibits a net magnetization due to the applied field. Since the states aligned parallel to the field are favored, the magnetization will enhance the exterior field and a paramagnetic contribution results.
For $T \approx 0$ both parabolas are essentially filled up to a sharp energy, and the net magnetization is simply given by the dark grey shaded region in Fig. 8.4c. Even for fields of the order of Tesla, the energetic shift of the states is $\mu_B\mu_0 H \sim 10^{-4}\,\text{eV}$, i.e. small on the scale of electronic energies. The shaded region representing our net magnetization can therefore be approximated by a simple rectangle of height $\mu_0\mu_B H$ and width $\frac{1}{2}N(\epsilon_F)$, i.e. the Fermi level DOS of the unperturbed system without applied field. We then have

$$N^{\uparrow} \;=\; \frac{N}{2} \;+\; \frac{1}{2}N(\epsilon_F)\mu_0\mu_B H \tag{8.51}$$

up electrons per volume and

$$N^{\downarrow} \;=\; \frac{N}{2} \;-\; \frac{1}{2}N(\epsilon_F)\mu_0\mu_B H \tag{8.52}$$

down electrons per volume. Since each electron contributes a magnetic moment of μ_B to the magnetization, we have

$$M \;=\; (N^{\uparrow} - N^{\downarrow})\mu_B \;=\; N(\epsilon_F)\mu_B^2\mu_0 H \tag{8.53}$$

(remember that the magnetization was the dipole magnetic density, and can in our uniform system therefore be written as dipole moment per electron times DOS). This then yields the susceptibility

$$\chi^{\text{mag,Pauli}} \;=\; \frac{\partial M}{\partial H} \;=\; \mu_0 \mu_B^2 N(\epsilon_F) \quad . \tag{8.54}$$

Using eq. (8.45) for the Fermi level DOS of the free electron gas, this can be rewritten as function of the Wigner-Seitz radius r_s

$$\chi^{\text{mag,Pauli}} \;=\; 10^{-6} \left(\frac{2.59}{r_s/a_B} \right) \quad . \tag{8.55}$$

Recalling that the Wigner-Seitz radius of most metals is of the order of 3-5 a_B, we find that the Pauli paramagnetic contribution ($\chi^{\text{mag,Pauli}} > 0$) of a free electron gas is small. In fact, as small as the diamagnetic susceptibility of atoms, and therefore much smaller than the paramagnetic susceptibility of atoms. For magnetic atoms in a material thermal disorder at finite temperatures prevents their complete alignment to an external field and therefore keeps the magnetism small. For an electron gas, on the other hand, it is the Pauli exclusion principle that opposes such an alignment by forcing the electrons to occupy energetically higher lying states when aligned. For the same reason, Pauli paramagnetism does not show the linear temperature dependence we observed in Curie's law in eq. (8.41). The characteristic temperature for the electron gas is the Fermi temperature. One could therefore cast the Pauli susceptibility into Curie form, but with a fixed temperature of order T_F playing the role of T. Since $T_F \gg T$, the Pauli susceptibility is then hundreds of times smaller and almost always completely negligible.
Turning to Landau diamagnetism, we note that its calculation would require solving the full quantum mechanical free electron problem along similar lines as done in the last section for atoms. The field-dependent Hamilton operator would then also produce a term that screens the applied field. Taking the second derivative of the resulting total energy with respect to **H**, one would obtain for the diamagnetic susceptibility

$$\chi^{\text{mag,Landau}} \;=\; -\frac{1}{3}\chi^{\text{mag,Pauli}} \quad , \tag{8.56}$$

i.e. another term that is as vanishingly small as the paramagnetic response of the free electron gas. Because this term is so small and the derivation does not yield new insight compared to the one already undertaken for the atomic case, we refer to e.g. the book by M.P. Marder, *Condensed Matter Physics* (Wiley, 2000) for a proper derivation of this result.

8.3.4 Atomic magnetism in solids

So far we have taken the tight-binding viewpoint of a material being an ensemble of atoms to understand its magnetic behavior. That is why we first addressed the magnetic properties of isolated atoms and ions. As an additional source of magnetism in solids we looked at free (delocalized) electrons. In both cases we found two major sources of magnetism: a paramagnetic one resulting from the alignment of existing "microscopic magnets" (either total angular momentum in the case of atoms, or spin in case of free electrons), and a diamagnetic one arising from induction currents trying to screen the external field.

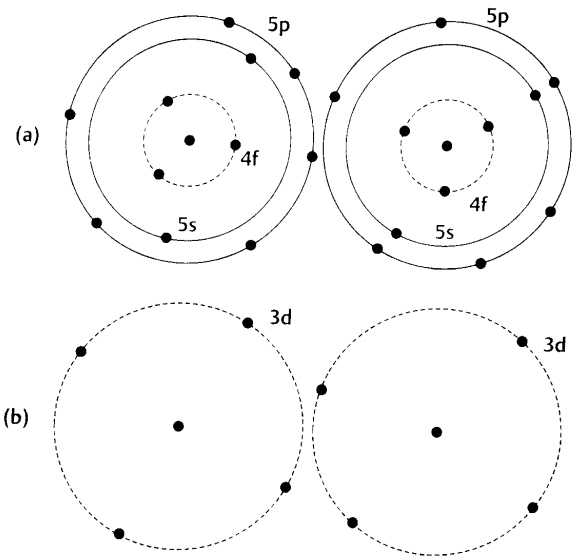

Figure 8.5: (a) In rare earth metal atoms the incomplete $4f$ electronic subshell is located inside the $5s$ and $5p$ subshells, so that the $4f$ electrons are not strongly affected by neighboring atoms. (b) In transition metal atoms, e.g. the iron group, the $3d$ electrons are the outermost electrons, and therefore interact strongly with other nearby atoms.

- Atoms (bound electrons):

- Paramagnetism	$\chi^{\text{mag,para}}$	$\approx 1/T \sim 10^{-2}\,(\text{RT})$	$\Delta E_0^{\text{para}} \sim 10^{-4}\,\text{eV}$
- Larmor diamagnetism	$\chi^{\text{mag,dia}}$	$\approx \text{const.} \sim -10^{-4}$	$\Delta E_0^{\text{dia}} \sim 10^{-9}\,\text{eV}$

- Free electrons:

- Pauli paramagnetism	$\chi^{\text{mag,Pauli}}$	$\approx \text{const.} \sim 10^{-6}$	$\Delta E_0^{\text{Pauli}} \sim 10^{-4}\,\text{eV}$
- Landau diamagnetism	$\chi^{\text{mag,Landau}}$	$\approx \text{const.} \sim -10^{-6}$	$\Delta E_0^{\text{Landau}} \sim 10^{-4}\,\text{eV}$

If the coupling between the different sources of magnetism is small, the magnetic behavior of the material would simply be a superposition of all relevant terms. For insulators this would imply, for example, that the magnetic moment of each atom/ion does not change appreciably when transfered to the material and the total susceptibility would be just the sum of all atomic susceptibilities. And this is indeed primarily what one finds when going through the periodic table:
Insulators: When $J = 0$, the paramagnetic contribution vanishes. If in addition $L = S = 0$ (closed-shell), the response is purely diamagnetic as in the case of noble gas solids or simple ionic crystals like the alkali halides (recall from the discussion on cohesion that the latter can be viewed as closed-shell systems!) or certain molecule (e.g. H_2O) and molecular crystals. Otherwise, the response is a balance between Van Vleck paramagnetism and Larmor diamagnetism. In all cases, the effects are small and the results from the theoretical derivation presented in the previous section are in excellent quantitative agreement with experiment.

d-count	# unpaired electrons		examples
	high spin	low spin	
d^4	4	2	Cr^{2+}, Mn^{3+}
d^5	5	1	Fe^{3+}, Mn^{2+}
d^6	4	0	Fe^{2+}, Co^{3+}
d^7	3	1	Co^{2+}

Table 8.3: High and low spin octahedral transition metal complexes.

More frequent is the situation $J \neq 0$, in which the response is dominated by the paramagnetic term. This is the case, when the material contains rare earth (RE) or transition metal (TM) ions (with partially filled f or d shells, respectively). These systems indeed obey Curie's law, i.e. they exhibit susceptibilities that scale inversely with temperature. For the rare earths, even the magnitude of the measured Curie constant corresponds very well to the theoretical one given by eq. (8.41). For TM ions in insulating solids, on the other hand, the measured Curie constant can only be understood by assuming $L = 0$, while S is still given by Hund's rules. This is referred to as *quenching of the orbital angular momentum* and is caused by a general phenomenon known as crystal field splitting. As illustrated by Fig. 8.5, the f orbitals of a RE atom are located deep inside the filled s and p shells and are therefore not significantly affected by the crystalline environment. On the contrary, the d shells of a TM atom belong to the outermost valence shells and are particularly sensitive to the environment. The crystal field lifts the 5-fold degeneracy of the TM d-states, as shown for an octahedral environment in Fig. 8.6a). Hund's rules are then in competition with the energy scale of the d-state splitting. If the energy separation is large only the three lowest states can be filled and Hund's rules give a low spin configuration with weak diamagnetism (Fig. 8.6b)). If the energy separation is small, Hund's rules can still be applied to all 5 states and a high spin situation with strong paramagnetism emerges (Fig. 8.6c)). The important thing to notice is, that although the solid perturbs the magnitude of the "microscopic magnet" connected with the partially filled shell, all individual moments inside the material are still virtually decoupled from each other (i.e. the magnetic moment in the material is that of an atom that has simply adapted to a new symmetry situation). This is why Curie's law is still valid, but the magnetic moment becomes an effective magnetic moment that depends on the crystalline environment. Table 8.3 summarizes the configurations for some transition metal ions in an octahedral environment.

Semiconductors: Covalent materials have only partially filled shells, so they could be expected to have a finite magnetic moment. However, covalent bonds form through a pair of electrons with opposite spin, and hence the net orbital angular momentum is zero. Covalent materials like Si (when they are not doped!!) exhibit therefore only a vanishingly small diamagnetic response. Dilute magnetic semiconductors, i.e. semiconductors doped with transition metal atoms, hold the promise to combine the powerful world of semiconductors with magnetism. However, questions like how pronounced the magnetism is and if room temperature magnetism can be achieved are still heavily debated and subject of an active research field.

Metals: In metals, the delocalized electrons add a new contribution to the magnetic behavior. In simple metals like the alkalis, this new contribution is in fact the only remaining

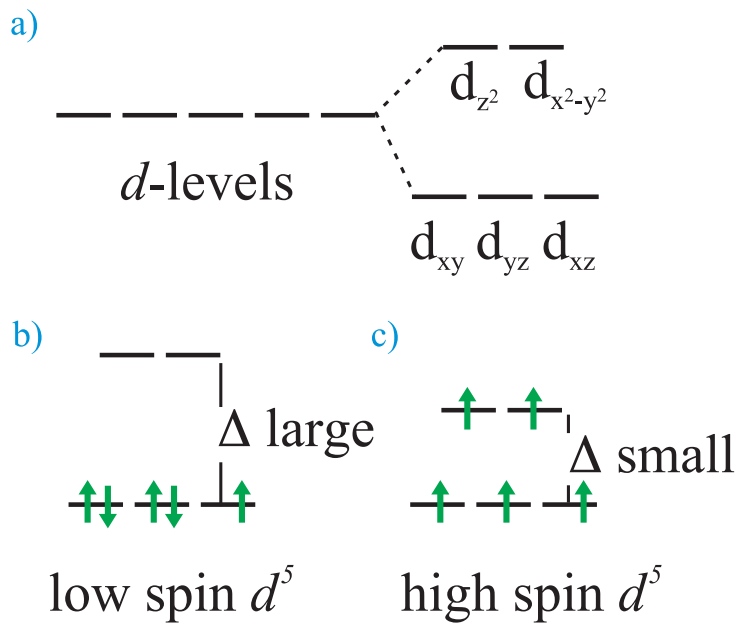

Figure 8.6: Effect of octahedral environment on transition metal ion with 5 electrons (d^5): a) the degenerate levels split into two groups, b) for large energy separation a low spin and for small energy separation a high spin configuration c) might be favorable.

one. As discussed in the chapter on cohesion, such metals can be viewed as closed-shell ion cores and a free electron glue formed from the valence electrons. The closed-shell ion cores have $J = L = S = 0$ and exhibit therefore only a negligible diamagnetic response. The magnetic behavior is then dominated by the Pauli paramagnetism of the conduction electrons. Measured susceptibilities are indeed of the order as expected from eq. (8.55), and the quantitative differences arise from the exchange-correlation effects that were not treated in our free electron model. More to come on metals below...

8.4 Magnetic order: Permanent magnets

The essence of the theory we have developed up to now is, that the magnetic properties of the majority of materials can be described entirely with the picture of atomic- and free-electron magnetism. In all cases, the paramagnetic or diamagnetic response is very small, at least when compared to electric susceptibilities, which are of the order of unity. This, by the way, is also the reason why typically only electric effects are discussed in the context of interactions with electromagnetic fields. At this stage, we could therefore close the chapter on magnetism of solids as something really unimportant, if it was not for a few elemental and compound materials (formed of or containing transition metal or rare earth atoms) that exhibit a completely different magnetic behavior: enormous susceptibilities and a magnetization that does not vanish when the external field is removed. Since such so-called *ferromagnetic effects* are not captured by the hitherto developed theory, they must originate from a strong coupling of the individual magnetic moments, which is what we will consider next.

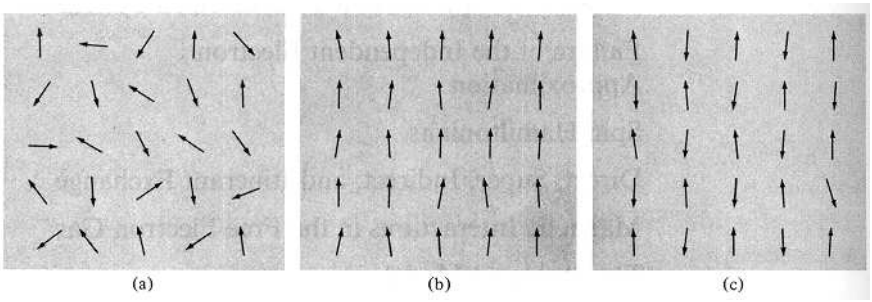

Figure 8.7: Schematic illustration of the distribution of directions of the local magnetic moments connected to "individual magnets" in a material. (a) random thermal disorder in a paramagnetic solid with insignificant magnetic interactions, (b) complete alignment either in a paramagnetic solid due to a strong external field or in a ferromagnetic solid below its critical temperature as a result of magnetic interactions. (c) Example of antiferromagnetic ordering below the critical temperature.

8.4.1 Ferro-, antiferro- and ferrimagnetism

The simple theory of paramagnetism in materials assumes that the individual magnetic moments (ionic shells of non-zero angular momentum in insulators or the conduction electrons in simple metals) do not interact with one another. In the absence of an external field, the individual magnetic moments are then thermally disordered at any finite temperature, i.e. they point in random directions yielding a zero net moment for the solid as a whole, cf. Fig. 8.7a. In such cases, an alignment can only be caused by an applied external field, which leads to an ordering of all magnetic moments at sufficiently low temperatures as schematically shown in Fig. 8.7b. However, a similar effect could also be obtained by coupling the different magnetic moments, i.e. by having an interaction that would favor a parallel alignment for example. Already quite short-ranged interactions, for example only between nearest neighbors, would already lead to an ordered structure as shown in Fig. 8.7b. Such interactions are often generically denoted as *magnetic interaction*, although this should not be misunderstood as implying that the source of interaction is really magnetic in nature (e.g. a magnetic dipole-dipole interaction, which in fact is not the reason for the ordering as we will see below).

Materials that exhibit an ordered magnetic structure in the absence of an applied external field are called *ferromagnets* (or permanent magnets), and their resulting (often nonvanishing) magnetic moment is known as *spontaneous magnetization* M_s. The complexity of the possible magnetically ordered states exceeds the simple parallel alignment case shown in Fig. 8.7b by far. In another common case the individual local moments sum to zero, and no spontaneous magnetization is present to reveal the microscopic ordering. Such magnetically ordered states are classified as *antiferromagnetic* and one possible realization is shown in Fig. 8.7c. If magnetic moments of different magnitude are present in the material, and not all local moments have a positive component along the direction of spontaneous magnetization, one talks about *ferrimagnets* ($M_\mathrm{s} \neq 0$). Fig. 8.8 shows a few examples of possible ordered structures. However, the complexity of possible magnetic structures is so large that some of them do not rigorously fall into any of the three categories. Those structures are well beyond the scope of this lecture and will not be covered here.

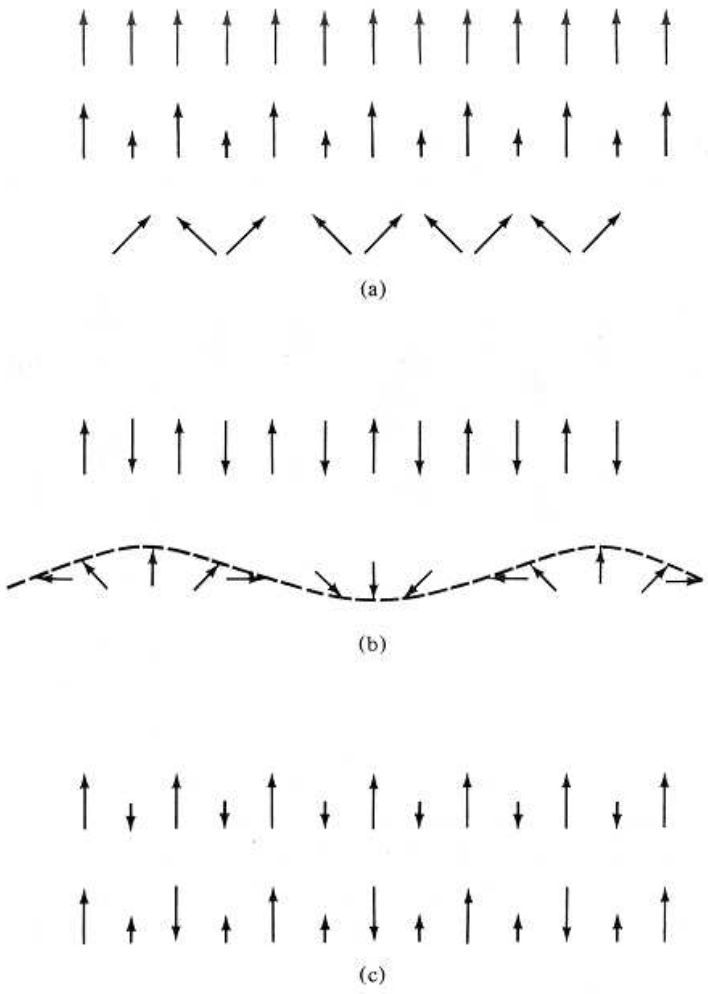

Figure 8.8: Typical magnetic orders in a simple linear array of spins. (a) ferromagnetic, (b) antiferromagnetic, and (c) ferrimagnetic.

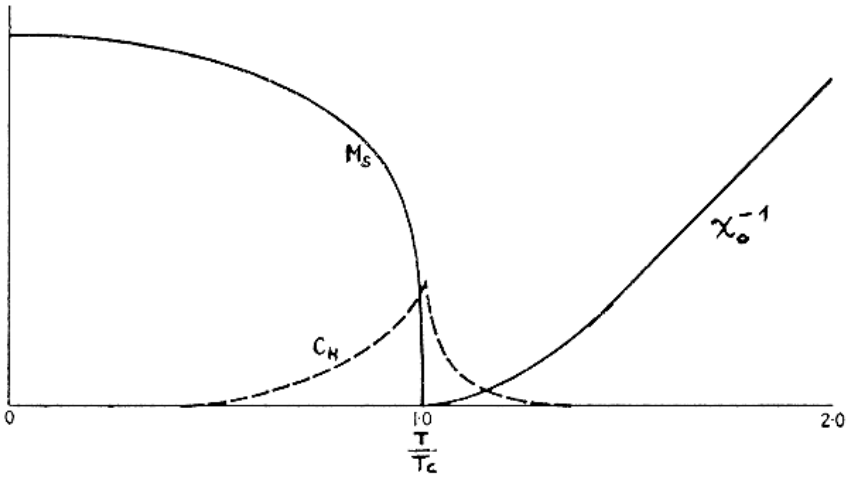

Figure 8.9: Typical temperature dependence of the magnetization M_s, the specific heat c_V and the zero-field susceptibility χ_o of a ferromagnet. The temperature scale is normalized to the critical (Curie) temperature T_c.

8.4.2 Interaction versus thermal disorder: Curie-Weiss law

Even in permanent magnets, the magnetic order does not usually prevail at all temperatures. Above a critical temperature T_c, the thermal energy can overcome the interaction induced order. The magnetic order vanishes and the material (often) behaves like a simple paramagnet. In ferromagnets, T_c is known as the *Curie temperature*, and in antiferromagnets as *Néel temperature* (sometimes denoted T_N). Note that T_c may depend strongly on the applied field (both in strength and direction!). If the external field is parallel to the direction of spontaneous magnetization, T_c typically increases with increasing external field, since both ordering tendencies support each other. For other field directions, a range of complex phenomena can arise as a result of the competition between both ordering tendencies.

At the moment we are, however, more interested in the ferromagnetic properties of materials in the absence of external fields, i.e. the existence of a finite spontaneous magnetization. The gradual loss of order with increasing temperature is reflected in the continuous drop of $M_s(T)$ as illustrated in Fig. 8.9. Just below T_c, a power law dependence is typically observed

$$M_s(T) \;\sim\; (T_c - T)^{\beta} \qquad (\text{for } \; T \to T_c^-) \quad , \tag{8.57}$$

with a critical exponent β somewhere around 1/3. Coming from the high temperature side, the onset of ordering also appears in the zero-field susceptibility, which is found to diverge as T approaches T_c

$$\chi_o(T) \;=\; \chi(T)|_{B=0} \;\sim\; (T - T_c)^{-\gamma} \qquad (\text{for } \; T \to T_c^+) \quad , \tag{8.58}$$

with γ around 4/3. This behavior already indicates that the material experiences dramatic changes at the critical temperature, which is also reflected by a divergence in other fundamental quantities like the zero-field specific heat

$$c_V(T)|_{B=0} \;\sim\; (T - T_c)^{-\alpha} \qquad (\text{for } \; T \to T_c) \quad , \tag{8.59}$$

	$\bar{m}_s$ (in μ_B)	m_{atom} (in μ_B)	T_c (in K)	Θ_c (in K)
Fe	2.2	6 (4)	1043	1100
Co	1.7	6 (3)	1394	1415
Ni	0.6	5 (2)	628	650
Eu	7.1	7	289	108
Gd	8.0	8	302	289
Dy	10.6	10	85	157

Table 8.4: Magnetic quantities of some elemental ferromagnets: The saturation magnetization at $T = 0\,\text{K}$ is given in form of the average magnetic moment $\bar{m}_s$ per atom and the critical temperature T_c and the Curie-Weiss temperature Θ_c are given in K. For comparison also the magnetic moment m_{atom} of the corresponding isolated atoms is listed (the values in brackets are for the case of orbital angular momentum quenching).

with α around 0.1. The divergence is connected to the onset of long-range order (alignment), which sets in more less suddenly at the critical temperature resulting in a second order phase transition. The actual transition is difficult to describe theoretically and theories are therefore often judged by how well (or badly) they reproduce the experimentally measured *critical exponents* α, β and γ.
Above the critical temperature, the properties of magnetic materials often become "more normal". In particular, for $T \gg T_c$, one usually finds a simple paramagnetic behavior, with a susceptibility that obeys the so-called *Curie-Weiss law*, cf. Fig. 8.9,

$$\chi_o(T) \;\sim\; (T - \Theta_c)^{-1} \qquad (\text{for } \; T \gg T_c) \quad . \tag{8.60}$$

Θ_c is called the Curie-Weiss temperature. Since γ in eq. (8.58) is almost never exactly equal to 1, Θ_c does not necessarily coincide with the Curie temperature T_c. This can, for example, be seen in Table 8.4, where also the saturated values for the spontaneous magnetization at $T \to 0\,\text{K}$ are listed.
In theoretical studies one typically converts this measured $M_s(T \to 0\,\text{K})$ directly into an average magnetic moment $\bar{m}_s$ per atom (in units of μ_B) by simply dividing by the atomic density in the material. In this way, we can compare directly with the corresponding values for the isolated atoms, obtained as $m_{\text{atom}} = g(JLS)\mu_B J$, cf. eq. (8.34). As apparent from Table 8.4, the two values agree very well for the rare earth metals, but differ substantially for the transition metals. Recalling the discussion on the quenching of the orbital angular momentum of TM atoms immersed in insulating materials in section 8.3.4, we could once again try to ascribe this difference to the symmetry lowering of interacting d orbitals in the material. Yet, even using $L = 0$ (and thus $J = S$, $g(JLS) = 2$), the agreement does not become much better, cf. Table 8.4. In the RE ferromagnets, the saturation magnetization appears to be a result of the perfect alignment of atomic magnetic moments that are not strongly affected by the presence of the surrounding material. The TM ferromagnets (Fe, Co, Ni), on the other hand, exhibit a much more complicated magnetic structure that is not well described by the magnetic behavior of the individual atoms.
As a first summary of our discussion on ferromagnetism (or ordered magnetic states in general) we are therefore led to conclude that it must arise out of an (yet unspecified) interaction between magnetic moments. This interaction produces an alignment of the magnetic moments, and subsequently a large net magnetization that prevails even in the

absence of an external field. This means we are certainly outside the linear response regime that has been our basis for developing the dia- and paramagnetic theories in the first sections of this chapter. With regard to the alignment, the interaction seems to have the same effect as an applied field acting on a paramagnet, which explains the similarity between the Curie-Weiss and the Curie law of paramagnetic solids: Interaction and external field favor alignment, and are opposed by thermal disorder. Below the critical temperature the alignment is perfect, and far above T_c the competition between alignment and disorder is equivalent to the situation in a paramagnet (just the origin of the temperature scale has shifted).
Sources for the interacting magnetic moments can be either delocalized electrons (Pauli paramagnetism) or partially filled atomic shells (Paramagnetism). This makes it plausible why ferromagnetism is a phenomenon specific to only some metals, and in particular metals with a high magnetic moment that arises from partially filled d or f shells (i.e. transition metals, rare earths, as well as their compounds). However, we cannot yet explain why only some and not all TMs and REs exhibit ferromagnetic behavior. The comparison between the measured values of the spontaneous magnetization and the atomic magnetic moments suggests that ferromagnetism in RE metals can be understood as the coupling of localized magnetic moments (due to the inert partially filled f shells). The situation is more complicated for TM ferromagnets, where the picture of a simple coupling between atomic-like moments fails. We will see below that this so-called *itinerant ferromagnetism* arises out of a subtle mixture of delocalized s electrons and the more localized, but nevertheless not inert d orbitals.

8.4.3 Phenomenological theories of ferromagnetism

After this first overview of phenomena arising out of magnetic order, let us now try to establish a proper theoretical understanding. Unfortunately, the theory of ferromagnetism is one of the less well developed of the fundamental theories in solid state physics (a bit better for the localized ferromagnetism of the REs, worse for the itinerant ferromagnetism of the TMs). The complex interplay of single particle and many-body effects, as well as collective effects and strong local coupling makes it difficult to break the topic down into simple models appropriate for an introductory level lecture. We will therefore not be able to present and discuss a full-blown *ab initio* theory like in the preceding chapters. Instead we will first consider simple phenomenological theories and refine them later, when needed. This will enable us to address some of the fundamental questions that are not amenable to phenomenological theories (like the source of the magnetic interaction).

8.4.3.1 Molecular (mean) field theory

The simplest phenomenological theory of ferromagnetism is the *molecular field theory* due to Weiss (1906). We had seen in the preceding section that the effect of the interaction between the discrete magnetic moments in a material is very similar to that of an applied external field (leading to alignment). For each magnetic moment, the net effect of the interaction with all other moments can therefore be thought of as a kind of internal field created by all other moments (and the magnetic moment itself). In this way we average over all interactions and condenses them into one effective field, i.e. molecular field theory is a typical representative of a *mean field theory*. Since this effective internal, or so-called

molecular field corresponds to an average over all interactions, it is reasonable to assume that it will scale with M, i.e. the overall magnetization (density of magnetic moments). Without specifying the microscopic origin of the magnetic interaction and the resulting field, the ansatz of Weiss was to simply postulate a linear scaling with M

$$H^{\text{mol}} \;=\; \mu_o \lambda M \quad , \tag{8.61}$$

where λ is the so-called molecular field constant. This leads to an effective field

$$H^{\text{eff}} \;=\; H + H^{\text{mol}} \;=\; H + \mu_o \lambda M \quad , \tag{8.62}$$

For simplicity, we will consider only the case of an isotropic material, so that the internal and the external point in the same direction, allowing us to write all formulae as scalar relations.
Recalling the magnetization of paramagnetic spins (Eq. 8.38)

$$M_0(T) = \frac{g(JLS)\mu_B J}{V} B_J(\eta) \quad \text{with} \eta \sim \frac{H}{T} \tag{8.63}$$

we obtain

$$M(T) = M_0 \left(\frac{H_{eff}}{T} \right) \rightarrow M_0 \left(\frac{\lambda M}{T} \right) \tag{8.64}$$

when the external field is switched off (H=0). We now ask the question if such a field can exist without an external field? Since M appears on the left and on the right hand side of the equation we perform a graphic solution. We set $x = \frac{\lambda}{T} M(T)$, which results in

$$M_0(x) = \frac{T}{\lambda} x \quad . \tag{8.65}$$

The graphic solution is show in Fig. 8.10 and tells us that the slop of $M_0(0K)$ has to be larger than $\frac{T}{\lambda}$. If this condition is fulfilled a ferromagnetic solution of our paramagnetic mean field model is obtained, although at this point we have no microscopic understanding of λ.
For the mean-field susceptibility we then obtain with $H(T) = M_0(\frac{H_{eff}}{T})$

$$\chi = \frac{\partial M_0}{\partial H} = \frac{\partial M_0}{\partial H_{eff}} \frac{\partial H_{eff}}{\partial H} = \frac{C}{T} \left(1 + \frac{\partial M}{\partial H} \right) = \frac{C}{T} \left(1 + \lambda \chi \right) \tag{8.66}$$

where we have used that for our paramagnet $\frac{\partial M_0}{\partial H_{eff}}$ is just Curie's law. Solving Eq. 8.66 for χ gives the Curie-Weiss law

$$\chi = \frac{C}{T - \lambda C} \sim \left(T - \Theta_c \right)^{-1} . \tag{8.67}$$

Θ_c is the Curie-Weiss temperature. The form of the Curie-Weiss law is compatible with an effective molecular field that scales linearly with the magnetization. Given the experimental observation of Curie-Weiss like scaling, the mean field ansatz of Weiss seems therefore reasonable. However, we can already see that this simple theory fails, as it predicts an inverse scaling with temperature for all $T > T_c$, i.e. within molecular field theory $\Theta_c = T_c$ and $\gamma = 1$ at variance with experiment. The exponent of 1, by the way, is characteristic for any mean field theory.

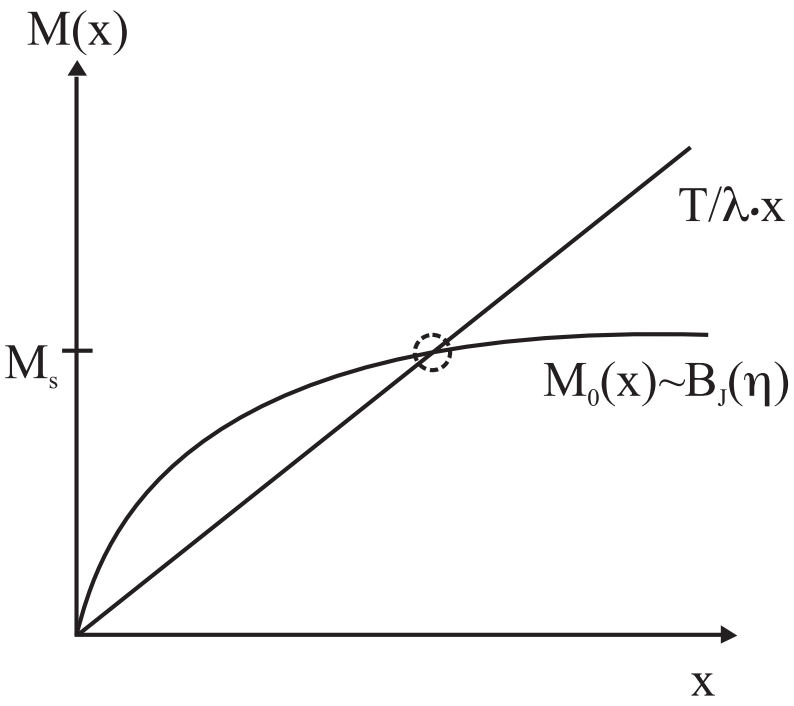

Figure 8.10: Graphical solution of equation 8.64.

Given the qualitative plausibility of the theory, let us nevertheless use it to derive a first order of magnitude estimate for this (yet unspecified) molecular field. This phenomenological consideration therefore follows the reverse logic to the *ab initio* one we prefer. In the latter, we would have analyzed the microscopic origin of the magnetic interaction and derived the molecular field as a suitable average, which in turn would have brought us into a position to predict materials' properties like the saturation magnetization and the critical temperature. Now, we do the opposite: We will use the experimentally known values of M_s and T_c to obtain a first estimate of the size of the molecular field, which might help us lateron to identify the microscopic origin of the magnetic interactions (about which we still do not know anything). For the estimate, recall that the Curie constant C was given by eq. (8.38) as

$$C \;=\; \frac{N\mu_o\mu_B^2 g(JLS)^2 J(J+1)}{3k_B V} \;\approx\; \left(\frac{N}{V}\right)\frac{\mu_o m_{\text{atom}}^2}{3k_B} \quad , \tag{8.68}$$

where we have exploited that $J(J+1) \sim J^2$, allowing us to identify the atomic magnetic moment $m_{\text{atom}} = \mu_B g(JLS)J$. With this, it is straightforward to arrive at the following estimate of the molecular field at $T = 0\,\text{K}$,

$$B^{\text{mol}}(0\,\text{K}) \;=\; \mu_o\lambda M_s(0\text{ K}) \;= \mu_o \frac{T_c}{C}\left(\frac{N}{V}\bar{m}_s\right) \approx \frac{3k_B T_c \bar{m}_s}{m_{\text{atom}}^2} \tag{8.69}$$

When discussing the content of Table 8.4 we had already seen that for most ferromagnets, m_{atom} is at least of the same order of $\bar{m}_s$, so that plugging in the numerical constants we arrive at the following order of magnitude estimate

$$B^{\text{mol}} \;\sim\; \frac{[5T_c \text{ in K}]}{[m_{\text{atom}} \text{ in } \mu_B]}\ \text{Tesla} \quad . \tag{8.70}$$

Looking at the values listed in Table 8.4, one realizes that molecular fields are of the order of some 10^3 Tesla, which is at least one order of magnitude more than the strongest magnetic fields that can currently be produced in the laboratory. As take-home message we therefore keep in mind that the magnetic interactions must be quite strong to yield such a high internal molecular field.
Molecular field theory can also be employed to understand the temperature behavior of the zero-field spontaneous magnetization. As shown in Fig. 8.9 $M_s(T)$ decays smoothly from its saturation value at $T = 0\,\mathrm{K}$ to zero at the critical temperature. Since the molecular field produced by the magnetic interaction is indistinguishable from an applied external one, the variation of $M_s(T)$ must be equivalent to the one of a paramagnet, only with the external field replaced by the molecular one. Using the results from section 8.3.2 for atomic paramagnetism, we therefore obtain directly a behavior equivalent to eq. (8.38)

$$M_s(T) \;=\; M_s(0\ \mathrm{K})\; B_J\!\left(\frac{g(JLS)\mu_B B^{\mathrm{mol}}}{k_B T}\right) \quad , \tag{8.71}$$

i.e. the temperature dependence is entirely given by the Brillouin function defined in eq. (8.39). $B_J(\eta)$, in fact, exhibits exactly the behavior we just discussed: it decays smoothly to zero as sketched in Fig. 8.9. Similar to the reproduction of the Curie-Weiss law, mean field theory provides us therefore with a simple rationalization of the observed phenomenon, but fails again on a quantitative level (and also does not tell us anything about the underlying microscopic mechanism). The functional dependence of $M_s(T)$ in both limits $T \to 0\,\mathrm{K}$ and $T \to T_c^-$ is incorrect, with e.g.

$$M_s(T \to T_c^-) \;\sim\; (T_c - T)^{1/2} \tag{8.72}$$

and thus $\beta = 1/2$ instead of the observed values around $1/3$. In the low temperature limit, the Brillouin function decays exponentially fast, which is also in gross disagreement with the experimentally observed $T^{3/2}$ behavior (known as *Bloch $T^{3/2}$ law*). The failure to predict the correct critical exponents is a general feature mean field theories that cannot account for the fluctuations connected with phase transitions. The wrong low temperature limit, on the other hand, is due to the non-existence of a particular set of low-energy excitations called spin-waves (or magnons), a point that we will come back to later.

8.4.3.2 Heisenberg and Ising Hamiltonian

Another class of phenomenological theories is called *spin Hamiltonians*. They are based on the hypothesis that magnetic order is due to the coupling between discrete microscopic magnetic moments. If these microscopic moments are, for example, connected to the partially filled f-shells of RE atoms, one can replace the material by a discrete lattice model, in which each site i has a magnetic moment $\mathbf{m}_i$. A coupling between two different sites i and j in the lattice can then be described by a term

$$H_{i,j}^{\mathrm{coupling}} \;=\; -\frac{J_{ij}}{\mu_B^2}\,\mathbf{m}_i \cdot \mathbf{m}_j \quad , \tag{8.73}$$

where J_{ij} is known as the exchange coupling constant between the two sites (unit: eV). In principle, the coupling can take any value between $-J_{ij}m_i m_j/\mu_B^2$ (parallel (ferromagnetic) alignment) and $+J_{ij}m_i m_j/\mu_B^2$ (antiparallel (antiferromagnetic) alignment) depending on

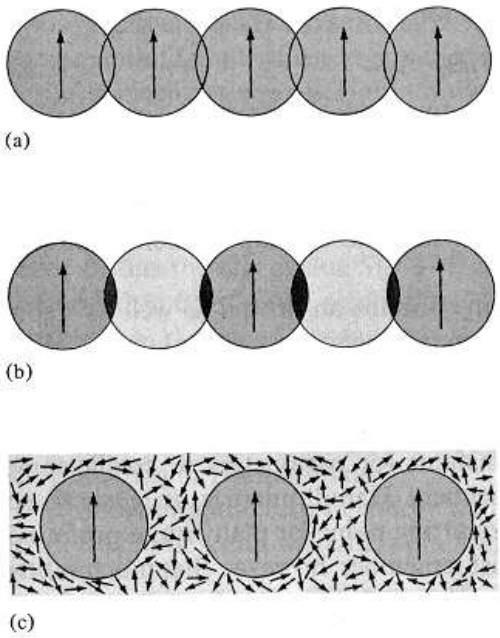

Figure 8.11: Schematic illustrations of possible coupling mechanisms between localized magnetic moments: (a) direct exchange between neighboring atoms, (b) superexchange mediated by non-magnetic ions, and (c) indirect exchange mediated by conduction electrons.

the relative orientation of the two moment vectors. Note that this simplified interaction has no explicit spatial dependence anymore. If this is required (e.g. in a non-isotropic crystal with a preferred magnetization axis), additional terms need to be added to the Hamiltonian.

Applying this coupling to the whole material, we first have to decide which lattice sites to couple. Since we are now dealing with a phenomenological theory we have no rigorous guidelines that would tell us which interactions are important. Instead, we have to choose the interactions (e.g. between nearest neighbors or up to next-nearest neighbors) and their strengths J_{ij}. Later, after we have solved the model, we can revisit these assumptions and see if they were justified. We can also use experimental (or first principles) data to fit the J_{ij}'s and hope to extract microscopic information. Often our choice is guided by intuition concerning the microscopic origin of the coupling. For the localized ferromagnetism of the rare earths one typically assumes a short-ranged interaction, which could either be between neighboring atoms (*direct exchange*) or reach across non-magnetic atoms in more complex structures (*superexchange*). As illustrated in Fig. 8.11 this conveys the idea that the interaction arises out of an overlap of electronic wavefunctions. Alternatively, one could also think of an interaction mediated by the glue of conduction electrons (*indirect exchange*), cf. Fig. 8.11c. However, without a proper microscopic theory it is difficult to distinguish between these different possibilities.

Having decided on the coupling, the Hamiltonian for the whole material becomes in its

simplest form of only pair-wise interactions

$$H^{\text{Heisenberg}} \;=\; \sum_{i,j=1}^{M} H_{i,j}^{\text{coupling}} \;=\; -\sum_{i,j=1}^{M} \frac{J_{ij}}{\mu_B^2}\, \mathbf{m}_i \cdot \mathbf{m}_j \quad . \tag{8.74}$$

Similar to the discussion in chapter 6 on cohesion, such a pairwise summation is only justified, when the interaction between two sites is not affected strongly by the presence of magnetic moments at other nearby sites. Since as yet we do not know anything about the microscopic origin of the interaction, this is quite hard to verify.
The particular spin Hamiltonian of eq. (8.74) is known as *Heisenberg Hamiltonian* and is the starting point for many theories of ferromagnetism. It looks deceptively simple, but in fact it is difficult to solve. Up to now, no analytic solution has been found. Since often analytic solutions are favored over numerical solutions further simplifications are made. Examples are one- or two-dimensional Heisenberg Hamiltonians (possibly only with nearest neighbor interaction) or the *Ising model*:

$$H^{\text{Ising}} \;=\; -\sum_{i,j=1}^{M} \frac{J_{ij}}{\mu_B^2}\, \underbrace{\mathbf{m}_{i,z} \cdot \mathbf{m}_{j,z}}_{\pm 1 \text{ only}} \quad . \tag{8.75}$$

These models opened up a whole field of research in the statistical mechanics community. It quickly developed a life of its own and became more and more detached from the original magnetic problem. Instead it was and is driven by the curiosity to solve the generic models themselves. In the meantime numerical techniques such as Monte Carlo developed that can solve the original Heisenberg Hamiltonian, although they do of course not reach the beauty of a proper analytical solution.
Since the Ising model has played a prominent role historically and because it has analytic solutions under certain conditions we will illustrate its solution in one dimension. For this we consider the Ising model in a magnetic field with only next nearest neighbor interactions

$$H^{\text{Ising}} \;=\; -\sum_{<ij>}^{M} J_{ij}\sigma_i\sigma_j - \sum_j h_j\sigma_j \tag{8.76}$$

where $< ij >$ denotes that the sum only runs over nearest neighbor and h_j is the magnetic field $\mu_0 H$ at site j and $\sigma_i = \pm 1$. Despite this simplified form no exact solution is known for the three dimensional case. For two dimensions Onsager found an exact solution in 1944 for zero magnetic field. Let us reduce the problem to one dimension and further simplify to $J_{i,i+1} = J$ and $h_j = h$:

$$H^{\text{Ising}} \;=\; -J\sum_{i=1}^{N} \sigma_i\sigma_{i+1} - h\sum_i \sigma_i \tag{8.77}$$

where we have used the periodic boundary condition $\sigma_{N+1} = \sigma_1$. The partition function for this Hamiltonian is

$$Z(N,h,T) = \sum_{\sigma_1} \cdots \sum_{\sigma_N} e^{\beta\left[J\sum_i^N \sigma_i\sigma_{i+1} + \frac{1}{2}\sum_i^N (\sigma_i + \sigma_{i+1})\right]} \tag{8.78}$$

with $\beta = \frac{1}{k_B T}$. In order to carry out the spin summation we define a matrix P:

$$< \sigma|P|\sigma' > = e^{\beta[J\sigma\sigma' + \frac{h}{2}(\sigma+\sigma')]} \tag{8.79}$$

$$< 1|P|1 > = e^{\beta[J+h]} \tag{8.80}$$

$$< -1|P|-1 > = e^{\beta[J-h]} \tag{8.81}$$

$$< 1|P|-1 > = < -1|P|1 > = e^{-\beta J} \tag{8.82}$$

$$\tag{8.83}$$

P is a 2×2 matrix called the transfer matrix

$$P = \begin{pmatrix} e^{\beta(J+h)} & e^{-\beta J} \\ e^{-\beta J} & e^{\beta(J-h)} \end{pmatrix} \quad . \tag{8.84}$$

With this definition the partition function becomes

$$Z(N,h,T) = \sum_{\sigma_1} \ldots \sum_{\sigma_N} < \sigma_1|P|\sigma_2 >< \sigma_2|P|\sigma_3 > \ldots < \sigma_{N-1}|P|\sigma_N >< \sigma_N|P|\sigma_1 > \tag{8.85}$$

$$= \sum_{\sigma_1} < \sigma_1|P^N|\sigma_1 > = Tr(P^N) \quad . \tag{8.86}$$

To evaluate the trace we have to diagonalize P, which yields the following eigenvalues

$$\lambda_\pm = e^{\beta J}\left[\cosh(\beta h) \pm \sqrt{\sinh^2(\beta h) + e^{-4\beta h}}\right] \quad . \tag{8.87}$$

With this the trace equates to

$$Tr(P^N) = \lambda_+^N + \lambda_-^N \quad . \tag{8.88}$$

Since we are interested in the thermodynamic limit $N \to \infty$, λ_+ will dominate over λ_-, because $\lambda_+ > \lambda_-$ for any h. This finally yields

$$Z(N,h,T) = \lambda_+^N \tag{8.89}$$

and gives us for the free energy per spin

$$F(h,T) = -k_B T \ln \lambda_+ = -J - \frac{1}{\beta} \ln\left[\cosh(\beta h) \pm \sqrt{\sinh^2(\beta h) + e^{-4\beta h}}\right] \quad . \tag{8.90}$$

The magnetization then follows as usual

$$M(h,T) = -\frac{\partial F}{\partial h} = \frac{\sinh(\beta h) + \frac{\sinh(\beta h)\cosh(\beta h)}{\sqrt{\sinh^2(\beta h) + e^{-4\beta h}}}}{\cosh(\beta h) + \sqrt{\sinh^2(\beta h) + e^{-4\beta h}}} \quad . \tag{8.91}$$

The magnetization is shown in Fig. 8.12 for different ratios J/h. For zero magnetic field ($h = 0$) $\coth(\beta h) = 1$ and $\sinh(\beta h) = 0$ and the magnetization vanishes. The next-nearest neighbor Ising model therefore does not yield a ferromagnetic solution in the absence of

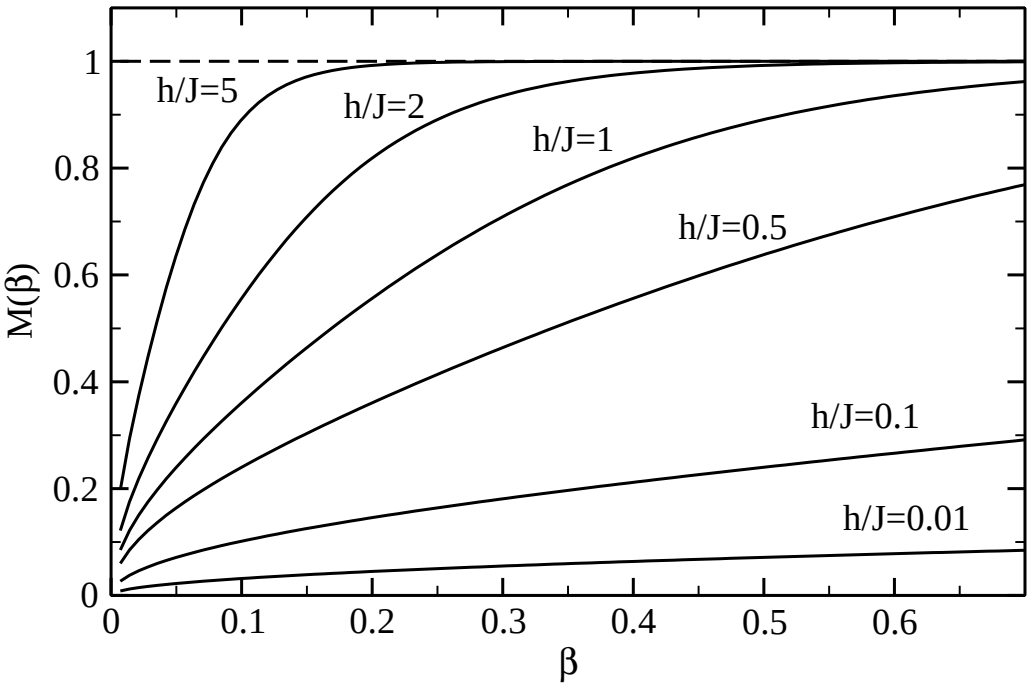

Figure 8.12: The magnetization $M(T)$ in the 1-dimensional Ising model as a function of inverse temperature $\beta = (k_B T)^{-1}$ for different ratios J/h.

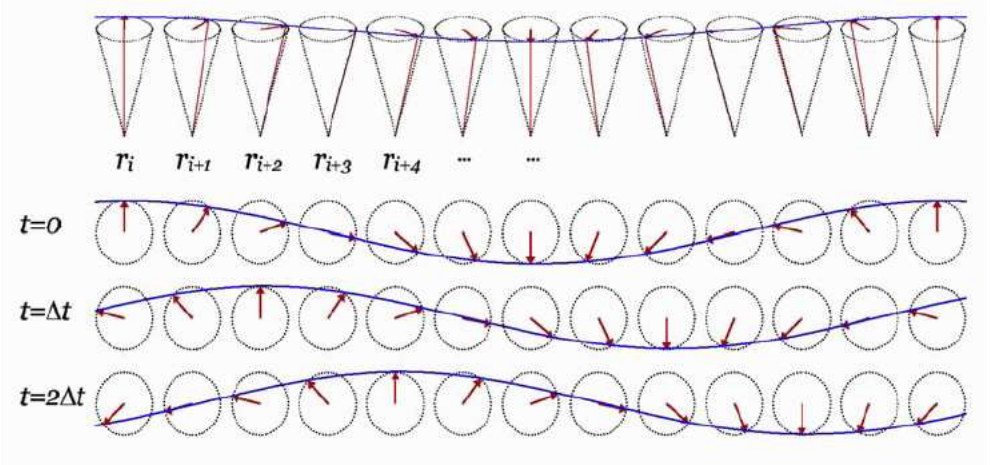

Figure 8.13: Schematic representation of the spatial orientation of the magnetic moments in a one-dimensional spin-wave.

a magnetic field. It also does not produce a ferromagnetic phase transition at finite field, unless the temperature is 0. The critical temperature for this model is thus zero Kelvin.

Returning now to the Heisenberg Hamiltonian, let us consider an elemental solid, in which all atoms are equivalent and exhibit the same magnetic moment $\mathbf{m}$. Inspection of eq. (8.74) reveals that $J > 0$ describes ferromagnetic and $J < 0$ antiferromagnetic coupling. The ferromagnetic ground state is given by a perfect alignment of all moments in one direction $|\uparrow\uparrow\uparrow \ldots \uparrow\uparrow>$. Naively one would expect the lowest energy excitations to be a simple spin flip $|\uparrow\downarrow\uparrow \ldots \uparrow\uparrow>$. Surprisingly, a detailed study of Heisenberg Hamiltonians reveals that these states not eigenstates of the Hamiltonian. Instead, the low energy excitations have a much more complicated wave-like form, with only slight directional changes between neighboring magnetic moments as illustrated in Fig. 8.13. At second thought it is then intuitive, that such waves will have only an infinitesimally higher energy than the ground state, if their wave vector is infinitely long. Such spin-waves are called *magnons*, and it is easy to see that they are missing from the mean-field description and also from the Ising model. As a result the Heisenberg Hamiltonian correctly accounts for the Bloch $T^{3/2}$-scaling of $M_s(T)$ for $T \to 0\,\mathrm{K}$. Magnons can in fact be expected quite generally, whenever there is a direction associated with the local order that can vary spatially in a continuous manner at an energy cost that becomes small as the wavelength of the variation becomes large. Magnons are quite common in magnetism (see e.g. the ground state of Cr) and their existence has been confirmed experimentally by e.g. neutron scattering.

The Heisenberg model also does a good job at describing other characteristics of ferromagnets. The high-temperature susceptibility follows a Curie-Weiss type law. Close to the critical temperature the solution deviates from the $1/T$-scaling. Monte Carlo simulations of Heisenberg ferromagnets yield critical exponents that are in very good agreement with the experimental data. Moreover, experimental susceptibility or spontaneous magnetization data can be used to fit the exchange constant J_{ij}. The values obtained for nearest neighbor interactions are typically of the order of $10^{-2}\,\mathrm{eV}$ for TM ferromagnets and $10^{-3} - 10^{-4}\,\mathrm{eV}$ for RE ferromagnets. These values are high compared to the energy splittings in dia- and paramagnetism and give us a first impression that the microscopic origin of ferromagnetic coupling must be comparatively strong.

We can also obtain this result by considering the mean-field limit of the Heisenberg Hamiltonian:

$$\begin{aligned} H^{\mathrm{Heisenberg}} &= -\sum_{i,j=1}^{M} \frac{J_{ij}}{\mu_B^2}\, \mathbf{m}_i \cdot \mathbf{m}_j \\ &= -\sum_{i=1}^{M} \mathbf{m}_i \cdot \left(\sum_{j=1}^{M} \frac{J_{ij}}{\mu_B^2} \mathbf{m}_j \right) \;=\; -\sum_{i=1}^{M} \mathbf{m}_i \cdot \mu_0 \mathbf{H_i} \quad . \end{aligned} \tag{8.92}$$

In the last step, we have realized that the term in brackets has the units of Tesla, and can therefore be perceived as a magnetic field $\mu_0\mathbf{H}$ arising from the coupling of moment i with all other moments in the solid. However, up to now we have not gained anything by this rewriting, because the effective magnetic field is different for every state (i.e. directional orientation of all moments). The situation can only be simplified, by assuming a mean field point of view and approximating this effective field by its thermal average $< \mathbf{H} >$.

This yields

$$\mu_0 < \mathbf{H} > = \sum_{j=1}^{M} \frac{J_{ij}}{\mu_B^2} < \mathbf{m}_j > = \frac{\sum_{j=1}^{M} J_{ij}}{\mu_B^2} \left(\frac{N}{V}\right) \mathbf{M}_s(T) \sim \lambda \mathbf{M}_s(T) \tag{8.93}$$

since the average magnetic moment at site i in an elemental crystal is simply given by the macroscopic magnetization (dipole moment density) divided by the density of sites. As apparent from eq. (8.93) we therefore arrive at a mean field that is linear in the magnetization as assumed by Weiss in his molecular field theory. In addition, we can now even relate the field to the microscopic quantity J_{ij}. If we assume for only nearest neighbor interactions in an fcc metal, it follows from eq. (8.93) that

$$J = J_{ij}^{NN} = \frac{\mu_B^2 B^{\text{mol}}}{12 \bar{m}_s} \quad . \tag{8.94}$$

Using the saturation magnetizations listed in Table 8.4 and the estimate of molecular fields of the order of 10^3 Tesla obtained above, we obtain exchange constants of the order of 10^{-2} eV for the TM or $10^{-3} - 10^{-4}$ eV for the RE ferromagnets in good agreement with the values mentioned before.

8.4.4 Microscopic origin of magnetic interaction

We have seen that the phenomenological models capture the characteristics of ferromagnetism. However, what is still lacking is microscopic insight into the origin of the strong interaction J. This must come from an *ab initio* theory. The natural choice (somehow also (falsely) conveyed by the name "magnetic interaction") is to consider the direct dipolar interaction energy of two magnetic dipoles $\mathbf{m}_1$ and $\mathbf{m}_2$, separated by a distance $\mathbf{r}$. For this, macroscopic electrodynamics gives us

$$J^{\text{mag dipole}} = \frac{1}{r^3} \left[\mathbf{m}_1 \cdot \mathbf{m}_2 - 3(\mathbf{m}_1 \cdot \hat{\mathbf{r}})(\mathbf{m}_2 \cdot \hat{\mathbf{r}})\right] \quad , \tag{8.95}$$

Omitting the angular dependence and assuming the two dipoles to be oriented parallel to each other and perpendicular to the vector between them we obtain the simplified expression

$$J^{\text{mag dipole}} \approx \frac{1}{r^3} m_1 m_2 \quad . \tag{8.96}$$

Inserting magnetic moments of the order of μ_B, cf. Table 8.4, and a typical distance of 2 Å between atoms in solids, this yields $J^{\text{mag dipole}} \sim 10^{-4}$ eV. This value is 1-2 orders of magnitude smaller than the exchange constants we derived using the phenomenological model in the previous section.

Having ruled out magnetic dipole interactions the only thing left are electrostatic (Coulomb) interactions. These do in fact give rise to the strong coupling, as we will see in the following. To be more precise it is the Coulomb interaction in competition with the *Pauli exclusion principle*. Loosely speaking, the exclusion principle keeps electrons with parallel spins apart, and thus reduces their Coulomb repulsion. The resulting difference in energy between the parallel spin configuration and the antiparallel one is the *exchange energy* we were seeking. This alignment is favorable for ferromagnetism only in exceptional circumstances because the increase in kinetic energy associated with parallel spins usually

outweighs the favorable decrease in potential energy. The difficulty in understanding magnetic ordering lies in the fact that we need to go beyond the independent electron (one particle) picture. In the next few sections, we will look at how the Pauli principle and the Coulomb interaction can lead to magnetic effects. We will do this for two simple yet opposite model cases: two localized magnetic moments and the free electron gas.

8.4.4.1 Exchange interaction between two localized moments

The most simple realization of two localized magnetic moments is the familiar problem of the hydrogen molecule. Here the two magnetic moments are given by the spins of the two electrons (1) and (2), which belong to the two H ions A and B. If there was only one ion and one electron, we would simply have the Hamiltonian of the hydrogen atom (h_o)

$$h_o|\phi> = \epsilon_o|\phi> \quad , \tag{8.97}$$

with its ground state solution $|\phi> = |\mathbf{r}, \sigma>$. For the molecule we then also have to consider the interaction between the two electrons and two ions themselves, as well as between the ions and electrons. This leads to the new Hamiltonian

$$H|\Phi> = (h_o(A) + h_o(B) + h_{\rm int})|\Phi> \quad , \tag{8.98}$$

where the two-electron wave function $|\Phi>$ is now a function of the positions of the ions A and B, the two electrons (1) and (2), and their two spins σ_1, σ_2. Since H has no explicit spin dependence, all spin operators commute with H and the total two-electron wave function must factorize

$$|\Phi> = |\Psi_{\rm orb}>|\chi_{\rm spin}> \quad , \tag{8.99}$$

i.e. into an orbital part and a pure spin part. As a suitable basis for the latter, we can choose the eigenfunctions of $\mathbf{S^2}$ and S_z, so that the spin part of the wave function is given by

$$\begin{array}{lll} |\chi_{\rm spin}>_{\rm S} = 2^{-1/2}\,(|\uparrow\downarrow> - |\downarrow\uparrow>) & S=0 & S_z=0 \\ |\chi_{\rm spin}>_{\rm T1} = |\uparrow\uparrow> & S=1 & S_z=1 \\ |\chi_{\rm spin}>_{\rm T2} = 2^{-1/2}\,(|\uparrow\downarrow> + |\downarrow\uparrow>) & S=1 & S_z=0 \\ |\chi_{\rm spin}>_{\rm T3} = |\downarrow\downarrow> & S=1 & S_z=-1 \quad . \end{array}$$

The fermionic character of the two electrons (and the Pauli exclusion principle) manifests itself at this stage in the general postulate that the two-electron wave function must change sign when interchanging the two indistinguishable electrons. $|\chi_{\rm spin}>_{\rm S}$ changes sign upon interchanging the two spins, while the three triplet wave functions $|\chi_{\rm spin}>_{\rm T}$ do not. Therefore only the following combinations are possible

$$\begin{aligned} |\Phi>_{\rm singlet} &= |\Psi_{\rm orb,sym}>\ |\chi_{\rm S}> \\ |\Phi>_{\rm triplet} &= |\Psi_{\rm orb,asym}>\ |\chi_{\rm T}> \quad , \end{aligned} \tag{8.100}$$

where $|\Psi_{\rm orb,sym}(1,2)> = |\Psi_{\rm orb,sym}(2,1)>$ and $|\Psi_{\rm orb,asym}(1,2)> = -|\Psi_{\rm orb,asym}(2,1)>$. This tells us that although the Hamiltonian of the system is spin independent a correlation between the spatial symmetry of the wave function and the total spin of the system emerges from the Pauli principle.

For the hydrogen molecule the full solution can be obtained numerically without too much difficulty. However, here we are interested in a solution that gives us insight and that allows us to connect to the Heisenberg picture. We therefore start in the fully dissociated limit of infinitely separated atoms ($< \Phi | h_{\rm int} | \Phi >= 0$). The total wave function must separate into a product of wave functions from the isolated H atoms

$$\phi_A(\mathbf{r}) = \frac{1}{\sqrt{N}} e^{-\alpha(\mathbf{r}-\mathbf{R}_A)} \quad . \tag{8.101}$$

However, the symmetry of the two electron wave function has to be maintained. Omitting the two ionic choices $\phi(1A)\phi(2A)$ and $\phi(1B)\phi(2B)$ that have a higher energy, the two low energy choices are

$$\begin{aligned} |\Psi^{\infty}_{\rm orb,sym}> &= 2^{-1/2} \left[\, |\phi(1A)>|\phi(2B)> \, + |\phi(2A)>|\phi(1B)> \, \right] \\ |\Psi^{\infty}_{\rm orb,asym}> &= 2^{-1/2} \left[\, |\phi(1A)>|\phi(2B)> \, - |\phi(2A)>|\phi(1B)> \, \right] \quad . \end{aligned} \tag{8.102}$$

Here $|\phi(1A)>$ is our notation for electron (1) being in orbit around ion A. These two wave functions correspond to the ground state of H_2 in either a spin singlet or a spin triplet configuration, and it is straightforward to verify that both states are degenerate in energy with $2\epsilon_o$.
Let us now consider what happens when we bring the two atoms closer together. At a certain distance, the two electron densities will slowly start to overlap and to change. Heitler and London made the following approximation for the two wave functions

$$\phi_A(\mathbf{r}) = \frac{1}{\sqrt{N}} e^{-\alpha \mathbf{r} \left(1+\beta \frac{\mathbf{r}\mathbf{R}_A}{r}\right)} \quad . \tag{8.103}$$

The two-electron problem is then still of the form given in eq. (8.102)

$$\begin{aligned} |\Psi^{\rm HL}_{\rm orb,sym}> &= (2+2S)^{-1/2} \left[\, |\phi(1A)>|\phi(2B)> \, + |\phi(2A)>|\phi(1B)> \, \right] \quad (8.104) \\ |\Psi^{\rm HL}_{\rm orb,asym}> &= (2-2S)^{-1/2} \left[\, |\phi(1A)>|\phi(2B)> \, - |\phi(2A)>|\phi(1B)> \, \right] \quad , \end{aligned}$$

where S is the overlap integral

$$S \; = < \phi(1A)|\phi(1B) >< \phi(2A)|\phi(2B) > = \; | < \phi(1A)|\phi(1B) > |^2 \quad . \tag{8.105}$$

Due to this change, the singlet ground state energy $E_{\rm S} =< \Phi|H|\Phi >_{\rm singlet}$ and the triplet ground state energy $E_{\rm T} =< \Phi|H|\Phi >_{\rm triplet}$ begin to deviate, and we obtain

$$E_{\rm T} - E_{\rm S} \; = \; 2 \, \frac{CS - A}{1 - S^2} \quad , \tag{8.106}$$

where

$$\begin{aligned} C &= < \phi(1A)| < \phi(2B)| \, H_{\rm int} \, |\phi(2B)>|\phi(1A)> \quad \text{(Coulomb integral)} \quad (8.107) \\ A &= < \phi(1A)| < \phi(2B)| \, H_{\rm int} \, |\phi(2A)>|\phi(1B)> \quad \text{(Exchange integral)} \quad (8.108) \end{aligned}$$

C is simply the Coulomb interaction of the two electrons with the two ions and themselves, while A arises from the exchange of the indistinguishable particles. If the exchange did not incur a sign change (as e.g. for two bosons), then $A = CS$ and the singlet-triplet

energy splitting would vanish. This tells us that it is the fermionic character of the two electrons that yields $A \neq CS$ as a consequence of the Pauli exclusion principle and in turn a finite energy difference between the singlet ground state (antiparallel spin alignment) and the triplet ground state (parallel spin alignment). For the H_2 molecule, the triplet ground state is in fact less energetically favorable, because it has an asymmetric orbital wave function. The latter must have a node exactly midway between the two atoms, meaning that there is no electron density at precisely that point where they could screen the Coulomb repulsion between the two atoms most efficiently. As we had anticipated, the coupling between the two localized magnetic moments is therefore the result of a subtle interplay of the electrostatic interactions and the Pauli exclusion principle. What determines the alignment is the availability of a spin state that minimizes the Coulomb repulsion between electrons once Fermi statistics has been taken into account. For this reason, magnetic interactions are also often referred to as *exchange interactions* (and the splitting between the corresponding energy levels as the *exchange splitting*).
By evaluating the two integrals C and A in eq. (8.108) using the one-electron wave functions of the H atom problem, we can determine the energy splitting $(E_\mathrm{T} - E_\mathrm{S})$. Realizing that the two level problem of the H_2 molecule can be also described by the Heisenberg Hamiltonian of eq. (8.74) (as we will show in the next section), we have therefore found a way to determine the exchange constant J. The Heitler-London approximation sketched in this section can be generalized to more than two magnetic moments, and is then one possible way for computing the exchange constants of Heisenberg Hamiltonians for (anti)ferromagnetic solids. However, this works only in the limit of highly localized magnetic moments, in which the wave function overlap is such that it provides an exchange interaction, but the electrons are not too delocalized (in which case the Heitler-London approximation of eq. (8.104) is unreasonable). With this understanding of the interaction between two localized moments, also the frequently used restriction to only nearest-neighbor interactions in Heisenberg Hamiltonians becomes plausible. As a note aside, in the extreme limit of a highly screened Coulomb interaction that only operates at each lattice site itself (and does not even reach the nearest neighbor lattice sites anymore), the magnetic behavior can also be described by a so-called *Hubbard model*, in which electrons are hopping on a discrete lattice and pay the price of a repulsive interaction U when two electrons of opposite spin occupy the same site.

8.4.4.2 From the Schrödinger equation to the Heisenberg Hamiltonian

Having gained a clearer understanding how the exchange interaction between two atoms arises we will now generalize this and derive a magnetic Hamiltonian from the Schrödinger equation. Recapping Chapter 0 the non-relativistic many-body Hamiltonian for the electrons is

$$H = -\sum_i \frac{\nabla^2}{2} - \sum_{ia} \frac{Z}{|\mathbf{r}_i - \mathbf{R}_a|} + \frac{1}{2}\sum_{ij} \frac{1}{|\mathbf{r}_i - \mathbf{r}_j|} \tag{8.109}$$

It is more convenient to switch to 2nd quantization by introducing the field operators

$$\psi(\mathbf{r}) = \sum_{\alpha,n,\lambda} \phi_{n\lambda}(\mathbf{r} - \mathbf{r}_\alpha) a_{n\lambda}(\mathbf{r}_\alpha), \tag{8.110}$$

where $a_{n\lambda}(\mathbf{r}_\alpha)$ annihilates an operator from state n and spin state λ at site $\mathbf{r}_\alpha$ and ϕ is the associated orbital. For the interaction part of the Hamiltonian we then obtain in 2nd

quantization

$$\frac{1}{2}\sum_{\substack{\alpha_1\alpha_2\alpha_3\alpha_4\\ n_1n_2n_3n_4\\ \lambda_1\lambda_2}} < \alpha_1 n_1 \alpha_2 n_2|V|\alpha_3 n_3 \alpha_4 n_4 > a^\dagger_{n_1\lambda_1}(\mathbf{r}_{\alpha_1}) a^\dagger_{n_2\lambda_2}(\mathbf{r}_{\alpha_2}) a_{n_3\lambda_2}(\mathbf{r}_{\alpha_3}) a_{n_4\lambda_1}(\mathbf{r}_{\alpha_4}) \quad . \tag{8.111}$$

This is still exact, but a bit unwieldy and not very transparent. Since the relevant orbitals are localized we can restrict the terms to those in which $\alpha_3 = \alpha_1$ and $\alpha_4 = \alpha_2$ or $\alpha_3 = \alpha_2$ and $\alpha_4 = \alpha_1$. The remaining terms involve various orbital excitations induced by the Coulomb interaction. These lead to *off-diagonal exchange*. We shall therefore restrict each electron to a definite orbital state. That is, we shall keep only those terms in which $n_3 = n_1$ and $n_4 = n_2$ or $n_3 = n_2$ and $n_4 = n_1$. If, for simplicity, we also neglect orbital-transfer terms, in which two electrons interchange orbital states, then the interaction part reduces to

$$\frac{1}{2}\sum_{\substack{\alpha\alpha'\\ nn'\\ \lambda\lambda'}} [< \alpha n \alpha' n'|V|\alpha n \alpha' n' > a^\dagger_{n\lambda}(\mathbf{r}_\alpha) a^\dagger_{n'\lambda'}(\mathbf{r}_{\alpha'}) a_{n'\lambda'}(\mathbf{r}_{\alpha'}) a_{n\lambda}(\mathbf{r}_\alpha) \tag{8.112}$$

$$+ < \alpha n \alpha' n'|V|\alpha' n' \alpha n >] \, a^\dagger_{n\lambda}(\mathbf{r}_\alpha) a^\dagger_{n'\lambda'}(\mathbf{r}_{\alpha'}) a_{n\lambda'}(\mathbf{r}_\alpha) a_{n'\lambda}(\mathbf{r}_{\alpha'}) \tag{8.113}$$

The first term is the direct and the second the exchange term that we encountered in the previous section. Using the fermion anticommutation relation

$$\left\{ a^\dagger_{n\lambda}(\mathbf{r}_\alpha) a_{n'\lambda'}(\mathbf{r}_{\alpha'}) = \delta_{\alpha\alpha'}\delta_{nn'}\delta_{\lambda\lambda'} \right\} \tag{8.114}$$

we may write the exchange term as

$$\frac{1}{2}\sum_{\substack{\alpha\alpha'\\ nn'\\ \lambda\lambda'}} J_{nn'}(\mathbf{r}_\alpha, \mathbf{r}_{\alpha'}) a^\dagger_{n\lambda}(\mathbf{r}_\alpha) a_{n\lambda'}(\mathbf{r}_\alpha) a^\dagger_{n'\lambda'}(\mathbf{r}_{\alpha'}) a_{n'\lambda}(\mathbf{r}_{\alpha'}) \quad . \tag{8.115}$$

Expanding the spin sums we can rewrite his

$$\frac{1}{2}\sum_{\substack{\alpha\alpha'\\ nn'\\ \lambda\lambda'}} J_{nn'}(\mathbf{r}_\alpha, \mathbf{r}_{\alpha'}) \left[\frac{1}{4} + \frac{1}{4}\mathbf{S}(\mathbf{r}_\alpha)\mathbf{S}(\mathbf{r}_{\alpha'}) \right], \tag{8.116}$$

where $\mathbf{S}$ is the spin (or magnetic moment) of the atom at site $\mathbf{r}_\alpha$. Now mapping over to lattice sites ($\mathbf{r}_\alpha \to i$ and $\mathbf{r}_{\alpha'} \to j$) we finally obtain the Heisenberg Hamiltonian from eq. (8.73)

$$H^{\rm spin} = \sum_{ij} \tilde{J}_{ij} \mathbf{S}_i \mathbf{S}_j \quad . \tag{8.117}$$

We have thus shown that magnetism does not arise from a spin-dependent part in the Schrödinger equation, but from the Pauli exclusion principle that the full many-body wave function has to satisfy. We could now use the Coulomb integrals derived in this section or the microscopic interaction we have derived in the previous section for J_{ij} to fill the Heisenberg Hamiltonian with life.

8.4.4.3 Exchange interaction in the homogeneous electron gas

The conclusion from the localized moment model is that feeding Heitler-London derived exchange constants into Hubbard or Heisenberg models provides a good semi-quantitative basis for describing the ferromagnetism of localized moments as is typical for rare earth solids. However, the other extreme of the more *itinerant ferromagnetism* found in the transition metals cannot be described. For this it is more appropriate to return to the homogeneous electron gas, i.e. treating the ions as a jellium background. We had studied this model already in section 8.3.3 for the independent electron approximation (zero electron-electron interaction) and found that the favorable spin alignment in an external field is counteracted by an increase in kinetic energy resulting from the occupation of energetically higher lying states. The net effect was weak and since there is no driving force for a spin alignment without an applied field we obtained a (Pauli) paramagnetic behavior.
If we now consider the electron-electron interaction, we find a new source for spin alignment in the exchange interaction, i.e. an exchange-hole mediated effect to reduce the repulsion of parallel spin states. This new contribution supports the ordering tendency of an applied field, and could (if strong enough) maybe even favor ordering in the absence of an applied field. To estimate whether this is possible, we consider the electron gas in the Hartree-Fock (HF) approximation as the minimal theory accounting for the exchange interaction. In the chapter on cohesion, we already derived the HF energy per electron, but without explicitly considering spins

$$(E/N)_{\text{jellium}} \;=\; T_s \;+\; E^{\text{XC}} \;\overset{HF}{\approx}\; \frac{30.1\,\text{eV}}{\left(\frac{r_s}{a_B}\right)^2} \;-\; \frac{12.5\,\text{eV}}{\left(\frac{r_s}{a_B}\right)} \quad . \tag{8.118}$$

Compared to the independent electron model of section 8.3.3, which only yields the first kinetic energy term, a second (attractive) term arises from exchange. To discuss magnetic behavior we now have to extend this description to the spin-polarized case. This is done in the most straightforward manner by rewriting the last expression as a function of the electron density (exploiting the definition of the Wigner-Seitz radius as $r_s/a_B = \left(\frac{3}{4\pi}(V/N)\right)^{1/3}$)

$$E_{\text{jellium,HF}}(N) \;=\; N\left\{78.2\,\text{eV}\left(\frac{N}{V}\right)^{2/3} \;-\; 20.1\,\text{eV}\left(\frac{N}{V}\right)^{1/3}\right\} \quad . \tag{8.119}$$

The obvious generalization to a spin-resolved gas is then

$$\begin{aligned} E^{\text{spin}}_{\text{jellium,HF}}(N^\uparrow, N^\downarrow) \;&=\; E_{\text{jellium,HF}}(N^\uparrow) \;+\; E_{\text{jellium,HF}}(N^\downarrow) \;= \\ &= \left\{78.2\,\text{eV}\left[\left(\frac{N^\uparrow}{V}\right)^{2/3} + \left(\frac{N^\downarrow}{V}\right)^{2/3}\right] \;-\; 20.1\,\text{eV}\left[\left(\frac{N^\uparrow}{V}\right)^{1/3} + \left(\frac{N^\downarrow}{V}\right)^{1/3}\right]\right\} \quad , \end{aligned} \tag{8.120}$$

where $N^\uparrow$ is the number of electrons with up spin, and $N^\downarrow$ with down spin ($N^\uparrow + N^\downarrow = N$). More elegantly, the effects of spin-polarization can be discussed by introducing the polarization

$$P \;=\; \frac{N^\uparrow - N^\downarrow}{N} \quad , \tag{8.121}$$

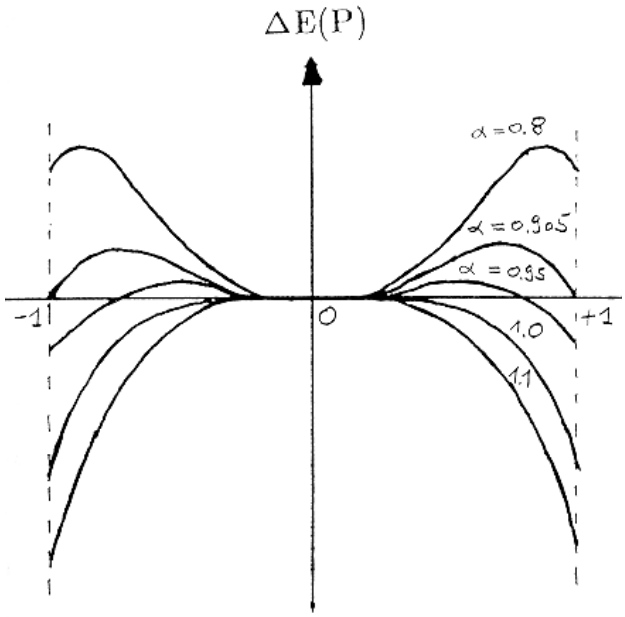

Figure 8.14: Plot of $\Delta E(P)$, cf. eq. (8.123), as a function of the polarization P and for various values of α. A ferromagnetic solution is found for $\alpha > 0.905$.

which possesses the obvious limits $P = \pm 1$ for complete spin alignment and $P = 0$ for a non-spinpolarized gas. Making use of the relations $N^{\uparrow} = \frac{N}{2}(1+P)$ and $N^{\downarrow} = \frac{N}{2}(1-P)$, eq. (8.120) can be cast into

$$E_{\text{jellium,HF}}(N,P) \;=\; NT\left\{\frac{1}{2}\left[(1+P)^{5/3}+(1-P)^{5/3}\right] \;-\; \frac{5}{4}\alpha\left[(1+P)^{4/3}+(1-P)^{4/3}\right]\right\} \quad , \tag{8.122}$$

with $\alpha = 0.10(V/N)^{1/3}$. Ferromagnetism, i.e. a non-vanishing spontaneous magnetization at zero field, can occur when a system configuration with $P \neq 0$ leads to a lower energy than the non-polarized case, $\Delta E(N,P) = E(N,P) - E(N,0) < 0$. Inserting the expression for the HF total energy we thus arrive at

$$\Delta E(N,P) \;=\; NT\left\{\frac{1}{2}\left[(1+P)^{5/3}+(1-P)^{5/3}-2\right] \;-\; \frac{5}{4}\alpha\left[(1+P)^{4/3}+(1-P)^{4/3}-2\right]\right\} \quad . \tag{8.123}$$

Figure 8.14 shows $\Delta E(N,P)$ as a function of the polarization P for various values of α. We see that the condition $\Delta E(N,P) < 0$ can only be fulfilled for

$$\alpha \;>\; \alpha_c \;=\; \frac{2}{5}(2^{1/3}+1) \;\approx\; 0.905 \quad , \tag{8.124}$$

in which case the lowest energy state is always given by a completely polarized gas ($P = 1$). Using the definition of α, this condition can be converted into a maximum electron density below which the gas possesses a ferromagnetic solution. In units of the Wigner-Seitz radius this is

$$\left(\frac{r_s}{a_B}\right) \;\gtrsim\; 5.45 \quad , \tag{8.125}$$

i.e. only electron gases with a density that is low enough to yield Wigner-Seitz radii above $5.6\,a_B$ would be ferromagnetic. Recalling that $1.8 < r_s < 5.6$ for real metals, only Cs would be a ferromagnet in the Hartree-Fock approximation.
Already this is obviously not in agreement with reality (Cs is paramagnetic and Fe/Co/Ni are ferromagnetic). However, the situation becomes even worse, when we start to improve the theoretical description by considering further electron exchange and correlation effects beyond Hartree-Fock. The prediction of the paramagnetic-ferromagnetic phase transition in the homogeneous electron gas has a long history, and the results vary dramatically with each level of exchange-correlation. The maximum density below which ferromagnetism can occur is, however, consistently obtained much lower than in eq. (8.125). The most quantitative work so far predicts ferromagnetism for electron gases with densities below $(r_s/a_B) \approx 50 \pm 2$ [F.H. Zhong, C.Lin, and D.M. Ceperley, Phys. Rev. B **66**, 036703 (2002)]. From this we conclude that Hartree-Fock theory allows us to qualitatively understand the reason behind itinerant ferromagnetism of delocalized electrons, but it overestimates the effect of the exchange interaction by one order of magnitude in terms of r_s. Yet, even a more refined treatment of electron exchange and correlation does not produce a good description of itinerant magnetism for real metals, none of which (with $1.8 < r_s < 5.6$) would be ferromagnetic at all in this theory. The reason for this failure cannot be found in our description of exchange and correlation, but must come from the jellium model itself. The fact that completely delocalized electrons (as in e.g. simple metals) cannot lead to ferromagnetism is correctly obtained by the jellium model, but not that Fe/Co/Ni are ferromagnetic. This results primarily from their partially filled d-electron shell, which is not well described by a free electron model as we had already seen in the chapter on cohesion. In order to finally understand the itinerant ferromagnetism of the transition metals, we therefore need to combine the exchange interaction with something that we have not yet considered at all: band structure effects.

8.4.5 Band consideration of ferromagnetism

In chapter 3 we had seen that an efficient treatment of electron correlation together with the explicit consideration of the ionic positions is possible within density-functional theory (DFT). Here, we can write for the total energy of the problem

$$E/N \;=\; T_s[n] + E^{\mathrm{ion-ion}}[n] + E^{\mathrm{el-ion}}[n] + E^{\mathrm{Hartree}}[n] + E^{\mathrm{XC}}[n] \quad , \tag{8.126}$$

where all terms are uniquely determined functions of the electron density $n(\mathbf{r})$. The most frequently employed approximation to the exchange-correlation term is the local density approximation (LDA), which gives the XC-energy at each point $\mathbf{r}$ as the one of the homogeneous electron gas with equivalent density $n(\mathbf{r})$. Recalling our procedure from the last section, it is straightforward to generalize to the so-called spin-polarized DFT, with

$$E/N \;=\; T_s[n^\uparrow, n^\downarrow] + E^{\mathrm{ion-ion}}[n] + E^{\mathrm{el-ion}}[n] + E^{\mathrm{Hartree}}[n] + E^{\mathrm{XC}}[n^\uparrow, n^\downarrow] \quad . \tag{8.127}$$

$n^\uparrow(\mathbf{r})$ and $n^\downarrow(\mathbf{r})$ then are the spin up and down electron densities, respectively. We only need to consider them separately in the kinetic energy term (since there might be a different number of up- and down- electrons) and in the exchange-correlation term. For the latter, we proceed as before and obtain the *local spin density approximation* (LSDA)

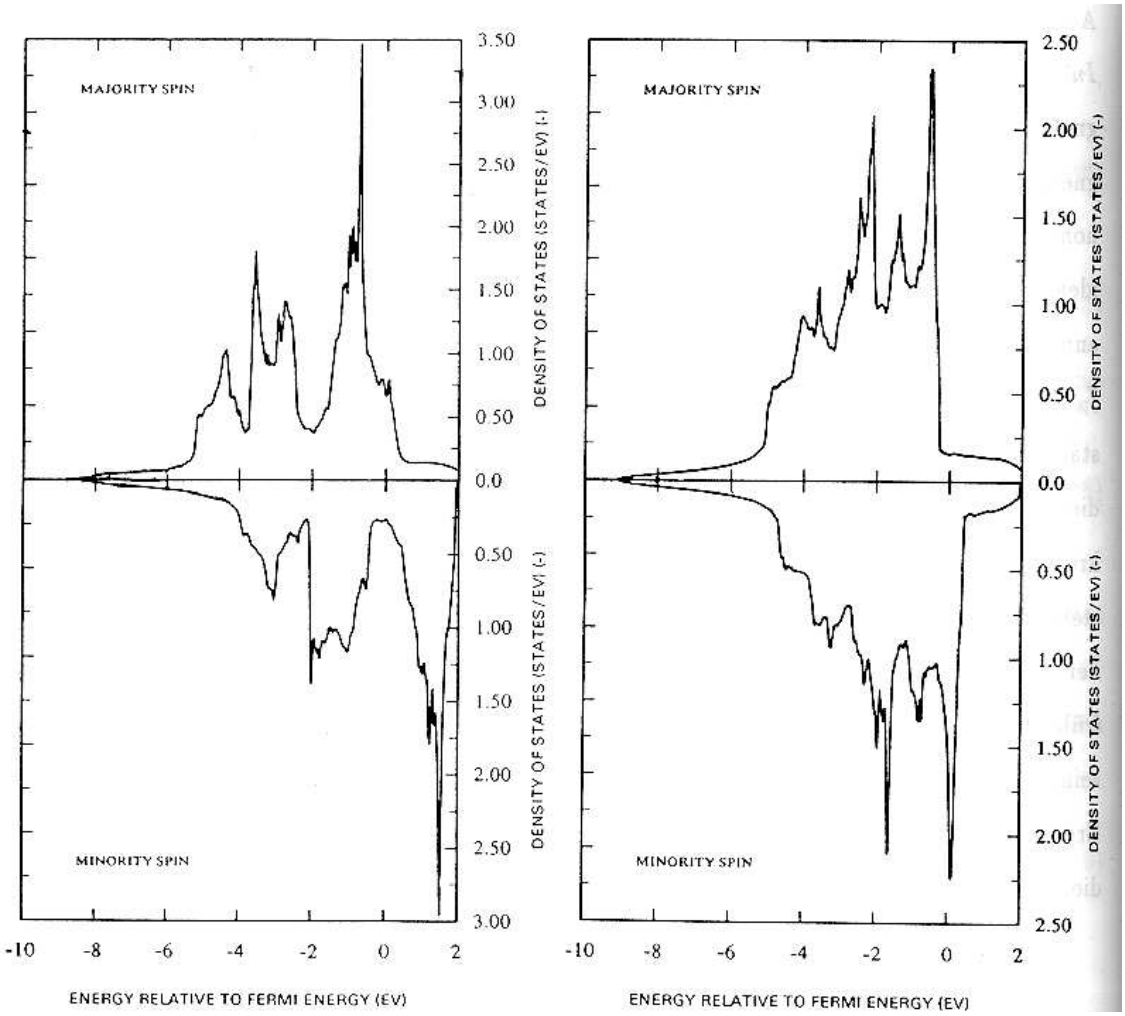

Figure 8.15: Spin-resolved density of states (DOS) for bulk Fe and Ni in DFT-LSDA [from V.L. Moruzzi, J.F. Janak and A.R. Williams, *Calculated electronic properties of metals*, Pergamon Press (1978)].

from the XC-energy of the spin-polarized homogeneous electron gas that we discussed in the previous section. Introducing the magnetization density

$$m(\mathbf{r}) \;=\; \left(n^{\uparrow}(\mathbf{r}) - n^{\downarrow}(\mathbf{r})\right)\mu_B \quad , \tag{8.128}$$

we can write the total energy as a function of $n(\mathbf{r})$ and $m(\mathbf{r})$. Since the integral of the magnetization density over the whole unit cell yields the total magnetic moment, self-consistent solutions of the coupled Kohn-Sham equations can then either be obtained under the constraint of a specified magnetic moment (*fixed spin moment (FSM) calculations*), or directly produce the magnetic moment that minimizes the total energy of the system.

Already in the LSDA this approach is very successful and yields a non-vanishing magnetic moment for Fe, Co, and Ni. Resulting spin-resolved density of states (DOS) for Fe and Ni are exemplified in Fig. 8.15. After self-consistency is reached, these three ferromagnetic metals exhibit a larger number of electrons in one spin direction (called majority

spin) than in the other (called minority spin). The effective potential seen by up and down electrons is therefore different, and correspondingly the Kohn-Sham eigenlevels differ (which upon filling the states up to a common Fermi-level yields the different number of up and down electrons that we had started with). Quantitatively one obtains in the LSDA the following average magnetic moments per atom, $\bar{m}_s = 2.1\ \mu_B$ (Fe), $1.6\ \mu_B$ (Co), and $0.6\ \mu_B$ (Ni), which compare excellently with the experimental saturated spontaneous magnetizations at $T = 0\,\mathrm{K}$ listed in Table 8.4. We can therefore state that DFT-LSDA reproduces the itinerant ferromagnetism of the elemental transition metals qualitatively and quantitatively! Although this is quite an achievement, it is still somewhat unsatisfying, because we do not yet *understand* why only these three elements in the periodic table exhibit ferromagnetism.

8.4.5.1 Stoner model of itinerant ferromagnetism

To derive at such an understanding, we take a closer look at the DOS of majority and minority spins in Fig. 8.15. Both DOS exhibit a fair amount of fine structure, but the most obvious observation is that the majority and minority DOS seem to be shifted relative to each other, but otherwise very similar. This can be rationalized by realizing that the magnetization density (i.e. the difference between the up and down electron densities) is significantly smaller than the total electron density itself. For the XC-correlation potential one can therefore write a Taylor expansion to first order in the magnetization density as

$$V_{\mathrm{XC}}^{\uparrow\downarrow}(\mathbf{r}) \;=\; \frac{\delta E_{\mathrm{XC}}^{\uparrow\downarrow}[n(\mathbf{r}), m(\mathbf{r})]}{\delta n(\mathbf{r})} \;\approx\; V_{\mathrm{XC}}^{0}(\mathbf{r}) \pm \tilde{V}(\mathbf{r}) m(\mathbf{r}) \quad , \tag{8.129}$$

where $V_{\mathrm{XC}}^{0}(\mathbf{r})$ is the XC-potential in the non-magnetic case. If the electron density is only slowly varying, one may assume the difference in up and down XC-potential (i.e. the term $\tilde{V}(\mathbf{r})m(\mathbf{r})$) to also vary slowly. In the *Stoner model*, one therefore approximates it with a constant term given by

$$V_{\mathrm{XC,Stoner}}^{\uparrow\downarrow}(\mathbf{r}) \;=\; V_{\mathrm{XC}}^{0}(\mathbf{r}) \pm \frac{1}{2} IM \quad . \tag{8.130}$$

The proportionality constant I is called the Stoner parameter (or exchange integral), and $M = \int_{unit-cell} m(\mathbf{r}) d\mathbf{r}$ (and thus $M = (\bar{m}_s/\mu_B)\times$ number of elements in the unit cell!). Since the only difference between the XC-potential seen by up and down electrons is a constant shift (in total: IM), the wave functions in the Kohn-Sham equations are not changed compared to the non-magnetic case. The only effect of the spin-polarization in the XC-potential is therefore to shift the eigenvalues $\epsilon_i^{\uparrow\downarrow}$ by a constant to lower or higher values

$$\epsilon_i^{\uparrow\downarrow} \;=\; \epsilon_i^{0} \;\pm\; 1/2 IM \quad . \tag{8.131}$$

The band structure and in turn the spin DOS are shifted with respect to the non-magnetic case,

$$N^{\uparrow\downarrow}(E) \;=\; \sum_i \int_{\mathrm{BZ}} \delta(E - \epsilon_{\mathbf{k},i}^{\uparrow\downarrow}) d\mathbf{k} \;=\; N^{0}(E \pm 1/2 IM) \quad , \tag{8.132}$$

i.e. the Stoner approximation corresponds exactly to our initial observation of a constant shift between the up and down spin DOS.

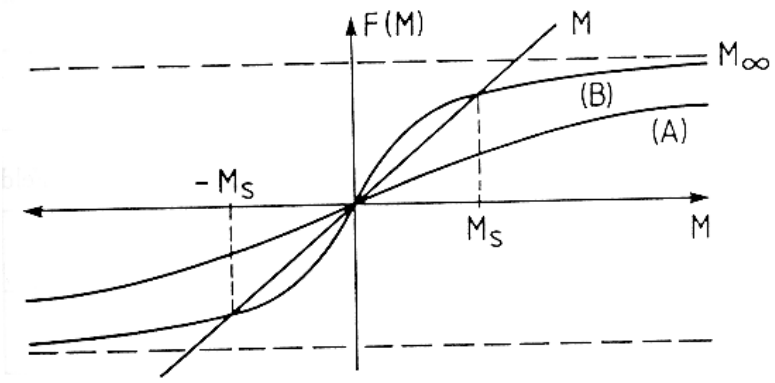

Figure 8.16: Graphical solution of the relation $M = F(M)$ of eq. (8.135) for two characteristic forms of $F(M)$.

So what have we gained by? So far nothing, but as we will see, we can employ the Stoner model to arrive at a simple condition that tells us by looking at an non-magnetic calculation, whether the material is likely to exhibit a ferromagnetic ground state or not. What we start out with are the results of a non-magnetic calculation, namely the non-magnetic DOS $N^0(E)$ and the total number of electrons N. In the magnetic case, N remains the same, but what enters as a new free variable is the magnetization M. In the Stoner model the whole effect of a possible spin-polarization is contained in the parameter I. We now want to relate M with I to arrive at a condition that tells us which I will yield a non-vanishing M (and thereby a ferromagnetic ground state). We therefore proceed by noticing that N and M are given by integrating over all occupied states of the shifted spin DOSs up to the Fermi-level

$$N = \int_{\epsilon_F} \left[N^0(E + 1/2IM) + N^0(E - 1/2IM)\right] dE \tag{8.133}$$

$$M = \int_{\epsilon_F} \left[N^0(E + 1/2IM) - N^0(E - 1/2IM)\right] dE \quad . \tag{8.134}$$

Since $N^0(E)$ and N are fixed, these two equations determine the remaining free variables of the magnetic calculation, ϵ_F and M. However, the two equations are coupled (i.e. they depend on the same variables), so that one has to solve them self-consistently. The resulting M is therefore characterized by self-consistently fulfilling the relation

$$M = \int_{\epsilon_F(M)} \left[N^0(E + 1/2IM) - N^0(E - 1/2IM)\right] dE \equiv F(M) \tag{8.135}$$

As expected M is a only function $F(M)$ of the Stoner parameter I, the DOS $N^0(E)$ of the non-magnetic material, and the filling of the latter (determined by ϵ_F and in turn by N). To really quantify the resulting M at this point, we would need an explicit knowledge of $N^0(E)$. Yet, even without such a knowledge we can derive some universal properties of the functional dependence of $F(M)$ that simply follow from its form and the fact that $N^0(E) > 0$,

$$F(M) = F(-M) \qquad\qquad F(0) = 0$$

$$F(\pm\infty) \;=\; \pm M_\infty \qquad\qquad F'(M) > 0 \quad .$$

Here M_∞ corresponds to the saturation magnetization at full spin polarization, when all majority spin states are occupied and all minority spin states are empty. The structure of $F(M)$ must therefore be quite simple: monotonously rising from a constant value at $-\infty$ to a constant value at $+\infty$, and in addition exhibiting mirror symmetry. Two possible generic forms of $F(M)$ that comply with these requirements are sketched in Fig. 8.16. In case (A), there is only the trivial solution $M = 0$ to the relation $M = F(M)$ of eq. (8.135), i.e. only a non-magnetic state results. In contrast, case (B) has three possible solutions. Apart from the trivial $M = 0$, two new solutions with a finite spontaneous magnetization $M = M_s \neq 0$ emerge. Therefore, if the slope of $F(M = 0)$ is larger than 1, the monotonous function $F(M)$ must necessarily cross the line M in another place, too. A sufficient criterion for the existence of ferromagnetic solutions with finite magnetization M_s is therefore $F'(0) > 1$.
Taking the derivative of eq. (8.135), we find that $F'(0) = IN^0(\epsilon_F)$, and finally arrive at the famous *Stoner criterion for ferromagnetism*

$$IN^0(\epsilon_F) \;>\; 1 \quad . \tag{8.136}$$

A sufficient condition for a material to exhibit ferromagnetism is therefore to have a high density of states at the Fermi-level and a large Stoner parameter. The latter is a material constant that can be computed within DFT (by taking the functional derivative of $V_{xc}^{\uparrow\downarrow}(\mathbf{r})$ with respect to the magnetization; see e.g. J.F. Janak, Phys. Rev. B **16**, 255 (1977)). Loosely speaking it measures the localization of the wave functions at the Fermi-level. In turn it represents the strength of the exchange interaction per electron, while $N^0(\epsilon_F)$ tells us how many electrons are able to participate in the ordering. Consequently, the Stoner criterion has a very intuitive form: strength per electron times number of electrons participating. If this exceeds a critical threshold, a ferromagnetic state results.
Figure 8.17 shows the quantities entering the Stoner criterion calculated within DFT-LSDA for all elements. Gratifyingly, only the three elements Fe, Co and Ni that are indeed ferromagnetic in reality fulfill the condition. With the understanding of the Stoner model we can now, however, also rationalize why it is only these three elements and not the others: For ferromagnetism we need a high number of states at the Fermi-level, such that only transition metals come into question. In particular, $N^0(\epsilon_F)$ is always highest for the very late TMs with an almost filled d-band. In addition, we also require a strong localization of the wave functions at the Fermi-level to yield a high Stoner parameter. And here, the compact $3d$ orbitals outwin the more delocalized ones of the $4d$ and $5d$ elements. Combining the two demands, only Fe, Co, and Ni remain.
Yet, it is interesting to see that also Ca, Sc and Pd come quite close to fulfilling the Stoner criterion. This is particularly relevant, if we consider other situations than the bulk. The DOSs of solids (although in general quite structured) scale to first order inversely with the band width W. In other words, the narrower the band, the higher the number of states per energy within the band. Just as much as by a stronger localization, W is also decreased by a lower coordination. In the atomic limit, the band width is zero and the Stoner criterion is always fulfilled. Correspondingly, all atoms with partially filled shells have a non-vanishing magnetic moment, given by Hund‘s rules. Somewhere intermediate are surfaces and thin films, where the atoms have a reduced coordination compared to

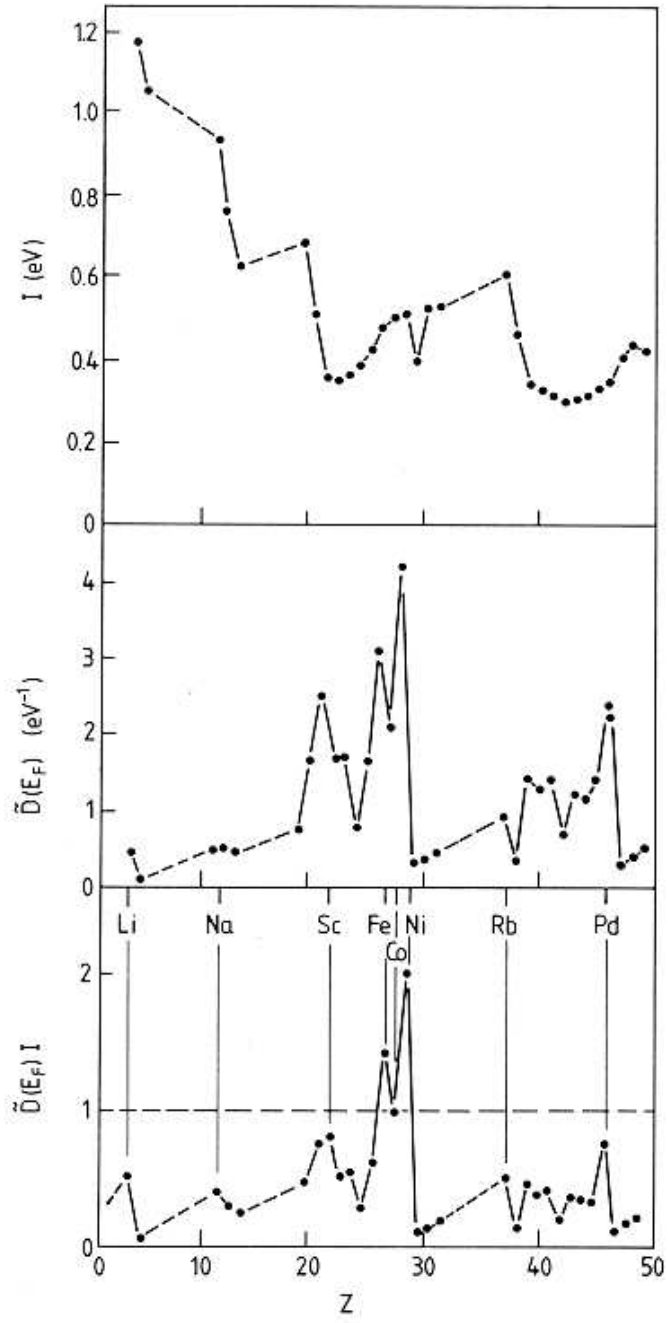

Figure 8.17: Trend over all elements of the Stoner parameter I, of the non-magnetic DOS at the Fermi-level (here denoted as $\tilde{D}(E_F)$) and of their product. The Stoner criterion is only fulfilled for the elements Fe, Co, and Ni [from H. Ibach and H. Lüth, *Solid State Physics*, Springer (1990)].

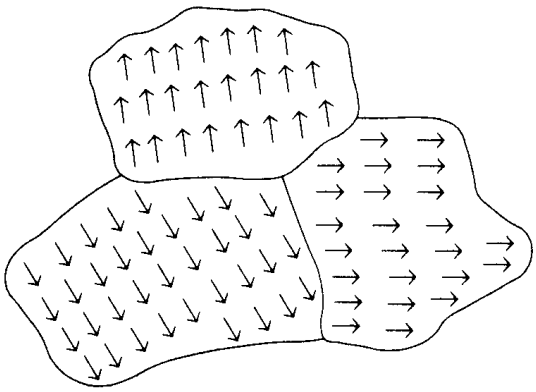

Figure 8.18: Schematic illustration of magnetic domain structure.

the bulk. The bands are then narrower and such systems can exhibit a larger magnetic moment or even a reversal of their magnetic properties (i.e. when they are non-magnetic in the bulk). The magnetism of surfaces and thin films is therefore substantially richer than the bulk magnetism discussed in this introductory lecture. Most importantly, it is also the basis of many technological applications.

8.5 Magnetic domain structure

With the results from the last section we can understand the ferromagnetism of the RE metals as a consequence of the exchange coupling between localized moments due to the partially filled (and mostly atomic-like) f-shells. The itinerant ferromagnetism of the TMs Fe, Co and Ni, on the other hand, comes from the exchange interaction of the still localized, but no longer atomic-like d orbitals together with the delocalized s-electron density. We can treat the prior localized magnetism using discrete Heisenberg or Hubbard models and exchange constants from Heitler-London type theories (or LDA+U type approaches), while the latter form of magnetism is more appropriately described within band theories like spin-DFT-LSDA. Despite this quite comprehensive understanding, an apparently contradictory feature of magnetic materials is that a ferromagnet does not always show a macroscopic net magnetization, even when the temperature is well below the Curie temperature. In addition it is hard to grasp, how the magnetization can be affected by external fields, when we know that the molecular internal fields are vastly larger.
The explanation for these puzzles lies in the fact that two rather different forces operate between the magnetic moments of a ferromagnet. At very short distance (of the order of atomic spacings), magnetic order is induced by the powerful, but quite short-ranged exchange forces. Simultaneously, at distances large compared with atomic spacings, the magnetic moments still interact as magnetic dipoles. We stressed in the beginning of the last section that the latter interaction is very weak; in fact between nearest neighbors it is orders of magnitude smaller than the exchange interaction. On the other hand, the dipolar interaction is rather long-ranged, falling off only as the inverse cube of the separation. Consequently, it can still diverge, if one sums over all interactions between a large population

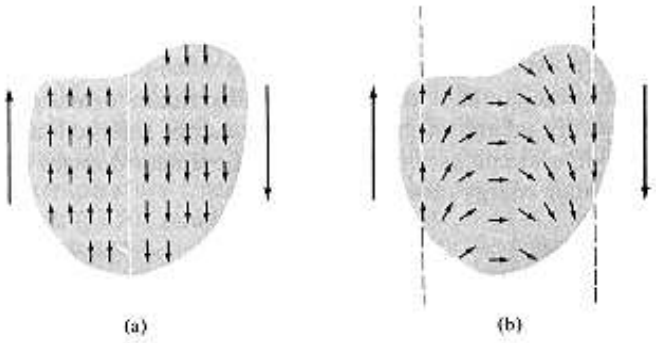

Figure 8.19: Schematic showing the alignment of magnetic moments at a domain wall with (a) an abrupt boundary and (b) a gradual boundary. The latter type is less costly in exchange energy.

that is uniformly magnetized. In order to accommodate these two competing interactions (short range alignment, but divergence if ordered ensembles become too large), ferromagnets organize themselves into *domains* as illustrated in Fig. 8.18. The dipolar energy is then substantially reduced, since due to the long-range interaction the energy of *every spin* drops. This bulk-like effect is opposed by the unfavorable exchange interactions with the nearby spins in the neighboring misaligned domains. Because, however, the exchange interaction is short-ranged, it is only the spins near the domain boundaries that will have their exchange energies raised, i.e. this is a surface effect. Provided that the domains are not too small, domain formation will be favored in spite of the vastly greater strength of the exchange interaction: Every spin can lower its (small) dipolar energy, but only a few (those near the domain boundaries) have their (large) exchange energy raised.

Whether or not a ferromagnet exhibits a macroscopic net magnetization, and how this magnetization is altered by external fields, has therefore less to do with creating alignment (or ripping it apart), but with the domain structure and how its size and orientational distribution is changed by the field. In this respect it is important to notice that the boundary between two domains (known as the domain wall or *Bloch wall*) has often not the (at first thought intuitive) abrupt structure. Instead a spread out, gradual change as shown in Fig. 8.19 is less costly in exchange energy. All an external field has to do then is to slightly affect the relative alignments (not flip one spin completely), in order to induce a smooth motion of the domain wall, and thereby increase the size of favorably aligned domains. The way how the comparably weak external fields can "magnetize" a piece of unmagnetized ferromagnet is therefore to rearrange and reorient the various domains, cf. Fig. 8.20. The corresponding domain wall motion can hereby be reversible, but it may also well be that it is hindered by crystalline imperfections (e.g. a grain boundary), through which the wall will only pass when the driving force due to the applied field is large. When the aligning field is removed, these defects may prevent the domain walls from returning to their original unmagnetized configuration, so that it becomes necessary to apply a rather strong field in the opposite direction to restore the original situation. The dynamics of the domains is thus quite complicated, and their states depend in detail upon the particular history that has been applied to them (which fields, how strong, which direction).

As a consequence, ferromagnets always exhibit so-called *hysteresis* effects, when plotting

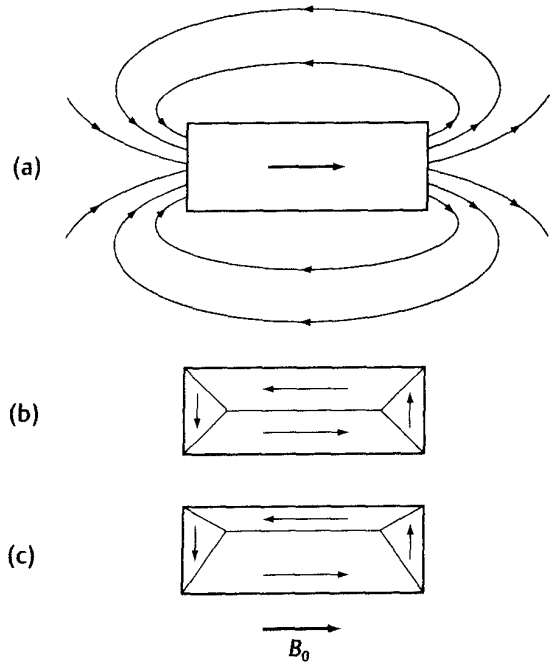

Figure 8.20: (a) If all of the magnetic moments in a ferromagnet are aligned they produce a magnetic field which extends outside the sample. (b) The net macroscopic magnetization of a crystal can be zero, when the moments are arranged in (randomly oriented) domains. (c) Application of an external magnetic field can move the domain walls so that the domains which have the moments aligned parallel to the field are increased in size. In total this gives rise to a net magnetization.

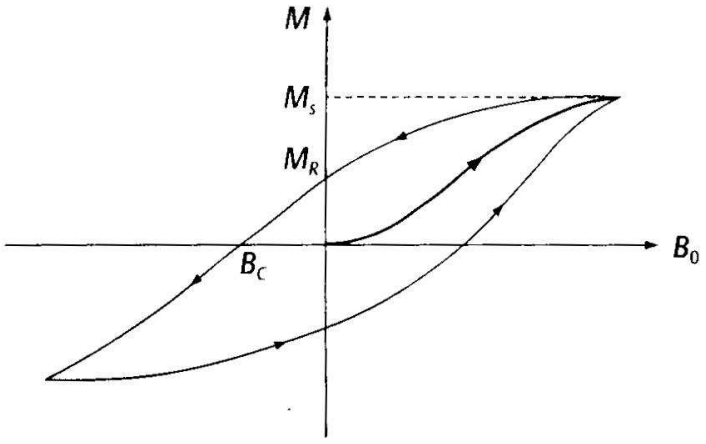

Figure 8.21: Typical hysteresis loop for a ferromagnet.

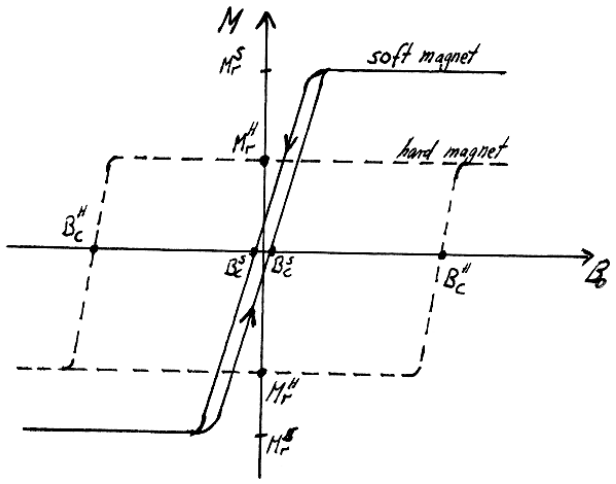

Figure 8.22: Hysteresis loops for soft and hard magnets.

the magnetization of the sample against the external magnetic field strength as shown in Fig. 8.21. Starting out with an initially unmagnetized crystal (at the origin), the applied external field induces a magnetization, which reaches a saturation value M_s when all dipoles are aligned. On removing the field, the irreversible part of the domain boundary dynamics leads to a slower decrease of the magnetization, leaving the so-called *remnant magnetization* M_R at zero field. One needs a reverse field (opposite to the magnetization of the sample) to further reduce the magnetization, which finally reaches zero at the so-called *coercive field* B_c.
Depending on the value of this coercive field, one distinguishes between *soft and hard magnets* in applications: A soft magnet has a small B_c and exhibits therefore only a small hysteresis loop as illustrated in Fig. 8.22. Such materials are employed, whenever one needs to reorient the magnetization frequently and without wanting to resort to strong fields to do so. Typical applications are kernels in engines, transformators, or switches and examples of soft magnetic materials are Fe or Fe-Ni, Fe-Co alloys. The idea of a hard magnet which requires a huge coercive field, cf. Fig. 8.22, is to maximally hinder the demagnetization of a once magnetized state. A major field of application is therefore magnetic storage with Fe- or Cr-Oxides, schematically illustrated in Fig. 8.23. The medium (tape or disc) is covered by many small magnetic particles each of which behaves as a single domain. A magnet – write head – records the information onto this medium by orienting the magnetic particles along particular directions. Reading information is then simply the reverse: The magnetic field produced by the magnetic particles induces a magnetization in the read head. In magnetoresistive materials, the electrical resistivity changes in the presence of a magnetic field so that it is possible to directly convert the magnetic field information into an electrical response. In 1988 a structure consisting of extremely thin, i.e. three atom-thick-alternative layers of Fe and Co was found to have a magnetoresistance about a hundred times larger than that of any natural material. This effect is known as *giant magnetoresistance* and is in the meanwhile exploited in todays disc drives.

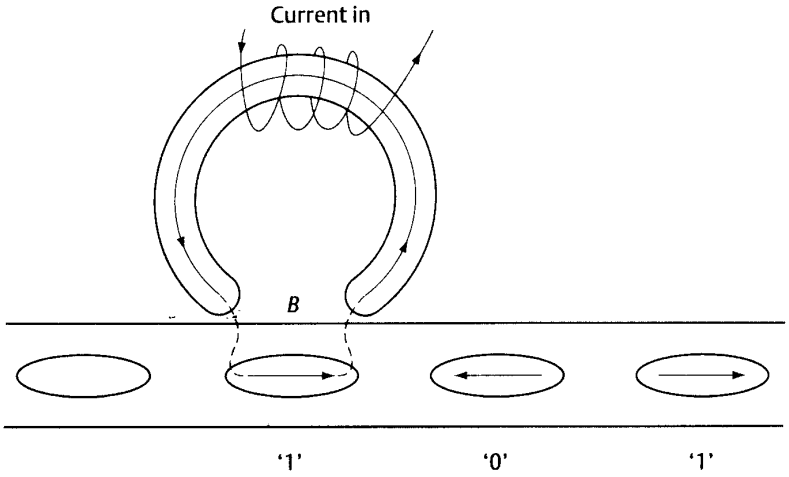

Figure 8.23: Illustration of the process of recording information onto a magnetic medium. The coil converts an electrical signal into a magnetic field in the write head, which in turn affects the orientation of the magnetic particles on the magnetic tape or disc. Here there are only two possible directions of magnetization of the particles, so the data is in binary form and the two states can be identified as 0 and 1.